Entanglement Dynamics and Applications Out of Thermal Equilibrium

Ansha Tayyab
Regn.# 364994

A thesis submitted in partial fulfillment of the requirements
for the degree of **Master of Science**

in

Physics

Supervised by: Dr. Muzzamal Iqbal Shaukat
Co-Supervised by: Dr. Aeysha Khalique

Department of Physics

School of Natural Sciences
National University of Sciences and Technology
H-12, Islamabad, Pakistan

2023

THESIS ACCEPTANCE CERTIFICATE

Certified that final copy of MS thesis written by **Ansha Tayyab** (Registration No. **00000364994)**, of **School of Natural Sciences** has been vetted by undersigned, found complete in all respects as per NUST statutes/regulations, is free of plagiarism, errors, and mistakes and is accepted as partial fulfillment for award of MS/M.Phil degree. It is further certified that necessary amendments as pointed out by GEC members and external examiner of the scholar have also been incorporated in the said thesis.

Signature: _____

Name of Supervisor: Dr. Muzzamal Iqbal Shaukat

Date: _____07/09/2023_____

Signature (HoD): _____

Date: ____07 – 09 – 2023____

Signature (Dean/Principal): _____

Date: ___07.09.2023___

National University of Sciences & Technology

MS THESIS WORK

We hereby recommend that the dissertation prepared under our supervision
by: Ansha Tayyab, Regn No. 00000364994 Titled: Entanglement Dynamics and
Applications Out of Thermal Equilibrium be Accepted in partial fulfillment of the
requirements for the award of **MS** degree.

Examination Committee Members

1. Name: DR. TAJAMMAL HUSSAIN   Signature:_____

2. Name: DR. SAADI ISHAQ   Signature:_____

Supervisor's Name DR. MUZZAMAL IQBAL
SHAUKAT   Signature:_____

Co Supervisor's Name DR. AEYSHA KHALIQUE   Signature: _____

_____
Head of Department

07-09-2023
Date

COUNTERSINGED

Date: 7.09.2023

_____
Dean/Principal

Dedication

Dedicated to Sajida Perveen, the best mother one could ever hope for, for your love that fills me with strength, the guidance that gives me ever-renewing curiosity and confidence, and unconditional support I sometimes don't deserve.

Acknowledgements

Abstract

Entanglement is a paramount attribute, used as a resource for several quantum applications. However, the desire to nip disentanglement in the bud is the topic to conversation among researchers. In this work, the creation of entanglement and steady state concurrence is reviewed for the quantum system out of thermal equilibrium and further the finite-time disentanglement is examined. To this aim, the Markovian master equation approach is employed to find the rate equations and Wootter's concurrence to analyze out-of-thermal equilibrium entanglement dynamics for coupled basis. The effect of super- and sub-radiant rates on entanglement sudden death is examined for different classes of X-states. It is found that the shorter dark period is achieved at a higher transition rate of a super-radiant state. Further the potentiality of superdense coding is examined and the dependence of superdense coding capacity on initial states for different ratios of sub- to super-radiant transition rates. The validity of dense coding is also analyzed for different probability amplitudes and it is perceived that maximally entangled states show the highest degree of coding capacity. This approach further allows us to analyze the applications of quantum information technologies

Contents

List of Figures

List of Tables

Chapter 1

Introduction

1.1 History

Late nineteenth century is marked with the essential composition of physics as classical mechanics, the concepts of electromagnetism and thermodynamics. Classical mechanics provides the formalism to study the effect of physical forces on the motion of bodies [1]. Maxwell's electromagnetism provides a complete framework to study the interaction between charged particles due to electromagnetic field [2]. In order to study matter-energy interactions the concepts of thermodynamics are used [3]. It was believed that all known physical phenomena could be explained with the help of these general concepts. Until, in 1900, series of queries start arising which could not be addressed using the existing framework of general theories. These queries pledge towards the birth of new era of physics, called modern physics [4]. The two main leads of modern physics was Maxwell's idea of quantum theory in 1900 and Einstein's formalism of special theory of relativity in 1905 [5]. These works was watershed in the history of physics. Einstein himself marked that period as *"It was a marvelous time to be alive"* [6].

Before 1900, the concept of light as electromagnetic rays was well established by Maxwell. At that time, classical mechanics seemed enough with little trouble in making sense with the nature of blackbody radiations [7] and photoelectric effect [6]. As far as Max Planck described light as a particle called "quanta". This definition of light assists to understand the concepts of blackbody radiation and photoelectric effect. The notion

of energy quantization leads towards compton effect and pair-production [6]. By 1913, Bohr explained the line spectrum of hydrogen by using the idea of quantization [8]. Later, Gilbert Lewis deduced the word "photon" to explain the particle-nature of wave [9].

After the experimental realization of wave-particle duality of light, de Broglie related this duality as the property of matter itself [10]. The triumphant contributions of Heisenberg, Schrödinger and Dirac hatch the basis of quantum mechanics. Heisenberg and Schrödinger introduced the two independent formalism to deal with quantum mechanics called *matrix mechanics* [11] and *wave mechanics* [12], respectively . On the other hand Dirac suggested the bra-ket notation. The bra-ket formalism is analogue to Heisenberg's matrix mechanics in discrete basis, while in continuous basis this formalism reimburse to Schrödinger's wave mechanics [13]. Later in 1927, Fermi and Dirac worked to analyze the concepts of quantum mechanics on fields instead of single particles, leading to quantum field theories (QFT) [14]. The year 1935 is marked with the new mystery in quantum mechanics, when Einstein along with Podolsky and Rosen (EPR) gives the concept of quantum correlations using Bell inequalities [15]. They proposed that there must be some *hidden variables* that fill the gap between intuitive condition of local action and quantum non-locality.

The quantum mechanics also provide theoretical explanation to the study of laser science, that rose interest in the field of quantum optics [16]. The contribution of Fermi and Dirac in QFT provides new insight to John R. Klauder et al., who worked to understand the concept of statistics of light, inaugurating the notion of coherent states [17] and squeezed states [7]. This knowledge pledges towards the discoveries of ultra-shot lasers pulses [18] using the technique of mode-locking [19] and Q-switching [20]. Other astonishing discoveries involve the concept of quantum correlations called quantum entanglement [21] and the applications of quantum optics in quantum information.

The benchmark of present day research involves the discoveries of quantum information theory (QIT). It combines the concepts of quantum mechanics [12], computer science [22] and information technology [23]. It uses the idea of quantum entanglement, which acts as a resource for many applications of QIT. These applications involve quantum

computing [24], quantum sensing, quantum cryptography [25], quantum key distribution [26], quantum teleportation [27], entanglement swapping [28] and superdense coding [29].

The discovery of the concepts of modern physics in twentieth century leads toward mysterious achievements in the technologies of modern world. Similarly, quantum mechanics provides a new insight of quantum world based on entanglement between quantum states. On the other hand, entanglement is a brittle phenomena that can easily dissipate on interacting with environment. A new development in the dissipation of entanglement was given by Yu and Eberly called finite-time disentanglement [30, 31, 32]. This astonishing phenomena gives the complete decay of entanglement within a finite period of time. At later time, the interaction between particles gives the revival of entanglement called entanglement sudden birth (ESB) [33].

1.2 Motivation

The desire to prevent entanglement in the open quantum systems has been a topic of engrossment among scientists. Such achievements include the reservoir engineering method [34, 35], experimental filtration of maximally entangled states from non-maximally entangled states [36], preserving entanglement through quantum Zeno effect [37] and entanglement mediated via plasmonic waveguides [38, 39]. However, the quantum system achieves thermal equilibrium at a later time, as a result, entanglement halts asymptotically. Therefore, all the approaches involved in preventing entanglement require an externally driven action to create steady entanglement [40]. Afterwards, efforts have been made to accomplish steady entanglement without any external assistance. Our motivation behind studying quantum system out of thermal equilibrium is to accomplish entanglement without any external aid. In such a system the thermal difference between a body placed closed to an emitter and its environment plays a role in achieving entanglement. Furthermore, nobody had studied how finite-time disentanglement can be manipulated for the quantum system out of thermal equilibrium. For that reason, in this thesis we studied the phenomena of finite-time disentangle-

ment and application of entanglement in super dense coding for different initial states. This approach further allows us to analyze the applications of quantum information technologies.

1.3 Objective and achievements

The main objective of this study is to boost the study of finite-time entanglement and super dense coding in quantum system out of thermal equilibrium. The scope of the present research can be outline in the following points:

- The dependence of finite-time disentanglement on probability amplitudes of initial states and other parameters including the effective number of photons in super- and sub-radiant states and also the transition rates of super- and sub-radiant states.

- The effect of super- and sub-radiant transition rates and their respective effective number of photons on super dense coding was examined for different classes of X-states.

To this aim, we employ the Markovian master equation approach to find the rate equations and Wootter's concurrence to analyze out-of-thermal equilibrium entanglement dynamics for coupled basis.

1.4 Structure of thesis

The thesis is structured into four chapters. The Chap. 2 of the thesis, "Fundamental Concepts" gives a fundamental overview of quantum tools and terminologies. The paramount goal is to equip the introduction and reference for the concepts involved in the thesis. Further in Chap. 3 we reviewed the creation of steady entanglement for the quantum system out of thermal equilibrium. While in Chap. 4 new insight for such quantum system is given by studying finite-time disentanglement and super dense coding for different X-states. Finally, in Chap. 5 the essence of the thesis is summarized and the obtained results and achievements of the thesis are highlighted.

Chapter 2

Fundamental Concepts

This chapter is equip with the basic concepts that will assist in understanding the phenomenons explained in further chapters. These basic concepts involve the definition of the building block of quantum information called qubit, the Bloch sphere representation of quantum states, the density operator approach and entangled state. Other concepts include the causes of decoherence counting brief introduction of finite-time disentanglement. In the second last section the main emphasis is on von Neumann entropy and Wootter's criteria to quantify entanglement. Lastly, super dense coding is briefly studied as an application of entanglement.

2.1 Qubit

A qubit is a two-level system epitomizing the simplest quantum system. For example, the spin of electron either up or down, polarization of light maybe vertically or horizontally polarized. It is a fundamental unit of quantum information. Alike classical bit, a qubit also has only two possible states but these states exist in superposition. Superposition is the linear combination of states until measurement is done, with no analogue in classical computation. On measurement, the superposition collapses into one of the state. In general, the state of a qubit in two-dimensional Hilbert space $\mathcal{H}$ is given as:

$$|\psi\rangle = \sum_i c_i |i\rangle .$$

(2.1)

Usually a normalized superposition state of a qubit in $\{0, 1\}$ basis is given as:

$$|\psi\rangle = \alpha |0\rangle + \beta |1\rangle, \tag{2.2}$$

with

$$|0\rangle = \begin{bmatrix} 1 \\ 0 \end{bmatrix}, \qquad\qquad |1\rangle = \begin{bmatrix} 0 \\ 1 \end{bmatrix}. \tag{2.3}$$

The coefficients α and β are the normalized probability amplitudes such that $|\alpha|^2 + |\beta|^2 = 1$. The measurement is performed on Eq. 2.2 such that, it will project the qubit on $\{|0\rangle, |1\rangle\}$ basis. As a result state $|0\rangle$ is obtained with probability $|\alpha|^2$ and state $|1\rangle$ is obtained with probability $|\beta|^2$. Here the basis set $\{|0\rangle, |1\rangle\}$ is called computational basis.

The superposition states for bipartite (two-qubit) system is given as the tensor product of both qubit's states. The Hilbert space for such state is $\mathcal{H}_1 \otimes \mathcal{H}_2$. Generally, the state of bipartite system can be written as:

$$|\psi\rangle_{12} = \sum_{ij} c_{ij} |i\rangle_1 \otimes |j\rangle_2. \tag{2.4}$$

It means that if $|i\rangle_1$ and $|j\rangle_2$ are the orthonormal basis for $\mathcal{H}_1$ and $\mathcal{H}_2$ respectively, then $|i\rangle \otimes |j\rangle$ is the orthonormal basis for $\mathcal{H}_1 \otimes \mathcal{H}_2$. For example, if states of two qubits are:

$$|\psi\rangle_1 = \alpha_1 |0\rangle + \beta_1 |1\rangle = \begin{bmatrix} \alpha_1 \\ \beta_1 \end{bmatrix}, \qquad |\psi\rangle_2 = \alpha_2 |0\rangle + \beta_2 |1\rangle = \begin{bmatrix} \alpha_2 \\ \beta_2 \end{bmatrix}, \tag{2.5}$$

then,

$$|\psi\rangle_{12} = |\psi\rangle_1 \otimes |\psi\rangle_2 = \alpha_1\alpha_2 |00\rangle + \alpha_1\beta_2 |01\rangle + \beta_1\alpha_2 |10\rangle + \beta_1\beta_2 |11\rangle = \begin{bmatrix} \alpha_1\alpha_2 \\ \alpha_1\beta_2 \\ \beta_1\alpha_2 \\ \beta_1\beta_2 \end{bmatrix}. \tag{2.6}$$

6

Here,

$$|00\rangle = |0\rangle \otimes |0\rangle = \begin{bmatrix} 1 \\ 0 \\ 0 \\ 0 \end{bmatrix}, |01\rangle = |0\rangle \otimes |1\rangle = \begin{bmatrix} 0 \\ 1 \\ 0 \\ 0 \end{bmatrix},$$

$$|10\rangle = |1\rangle \otimes |0\rangle = \begin{bmatrix} 0 \\ 0 \\ 1 \\ 0 \end{bmatrix}, |11\rangle = |1\rangle \otimes |1\rangle = \begin{bmatrix} 0 \\ 0 \\ 0 \\ 1 \end{bmatrix}. \tag{2.7}$$

The same is true for n-number of qubits, a general superposition state of n-qubits is the tensor product of 2^n states. Similarly the Hilbert space of n-number of qubits is the tensor product of each qubit's Hilbert space.

2.2 Bloch sphere

Another representation of qubit state is given as:

$$|\psi\rangle = cos\theta/2 |0\rangle + e^{i\phi} sin\theta/2 |1\rangle = \begin{bmatrix} cos\theta/2 \\ e^{i\phi} sin\theta/2 \end{bmatrix}. \tag{2.8}$$

The depection of qubit state in Eq. 2.8 gives a prespective of bloch sphere representation. Bloch sphere renders geometric representation of all possible states of qubit. The north and south poles of the sphere usually represent the standard basis $|0\rangle$ and $|1\rangle$. However, the points on the sphere's surface represents the pure states, while the inner points give mixed state and the central point is marked with totally mixed state. It is a three-dimensional unit sphere embedded in the Cartesian coordinates ($n_x = cos\phi sin\theta$, $n_y = sin\phi sin\theta$, $n_z = cos\theta$). Thus any quantum state on Bloch sphere is defined by θ and ϕ representing a unique Bloch vector $\hat{n} = (n_x, n_y, n_z)$. The generic state given in Eq. 2.8 can be written as

$$|\psi\rangle = \frac{1}{\sqrt{2}} \begin{bmatrix} \sqrt{1+n_z} \\ \frac{n_x + in_y}{\sqrt{1+n_z}} \end{bmatrix}. \tag{2.9}$$
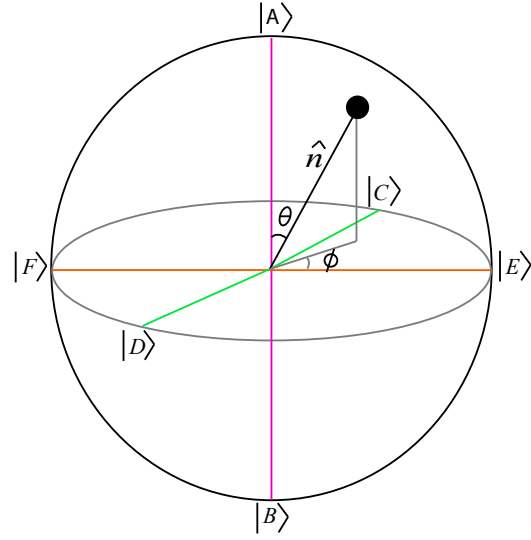
Figure 2.1: Bloch sphere representation of different Bloch vectors. Here $\hat{n}$ is a general Block sphere vector.

As an example consider the points A, B, C, D, E and F on a Bloch sphere. These points are given as:

$$
\begin{aligned}
\hat{A} &= (0,0,1), & |A\rangle &= \begin{bmatrix} 1 \\ 0 \end{bmatrix}, \\
\hat{B} &= (0,0,-1), & |B\rangle &= \begin{bmatrix} 0 \\ 1 \end{bmatrix}, \\
\hat{C} &= (-1,0,0), & |C\rangle &= \frac{1}{\sqrt{2}} \begin{bmatrix} 1 \\ -1 \end{bmatrix}, \\
\hat{D} &= (1,0,0), & |D\rangle &= \frac{1}{\sqrt{2}} \begin{bmatrix} 1 \\ 1 \end{bmatrix}, \\
\hat{E} &= (0,1,0), & |E\rangle &= \frac{1}{\sqrt{2}} \begin{bmatrix} 1 \\ i \end{bmatrix}, \\
\hat{F} &= (0,-1,0), & |F\rangle &= \frac{1}{\sqrt{2}} \begin{bmatrix} 1 \\ -i \end{bmatrix}.
\end{aligned}
\tag{2.10}
$$

Thus, any vector on Bloch sphere can be represented using a Bloch vector.

2.3 Density operator

The density operator is used as a substitute for the physical representation of quantum state. A wavefunction representation is only valid for pure states. In order to represent the statistical ensemble of pure states called mixed state, the density operator is used. It is defined as the outer product of wavefunction. For the general state given in Eq. 2.1, it is written as:

$$\rho = |\psi\rangle\langle\psi| = \sum_i p_i |i\rangle\langle i|. \tag{2.11}$$

Here $p_i = |c_i|^2$ gives the probability amplitude corresponding to state i. It must satisfy the general properties of probability i.e.,

$$0 \leq p_i \leq 1, \qquad \sum_i p_i = 1, \qquad \sum_i p_i^2 \leq 1. \tag{2.12}$$

For the special case of pure state, the probability of all other states vanish except for one state, suppose it is state k. Thus, the density operator for pure state becomes a projector operator:

$$\rho = |k\rangle\langle k|. \tag{2.13}$$

2.3.1 Properties of density operator

The density operator satisfies the following properties:

- The density operator ρ is hermitian. It means:

$$\begin{aligned}
\rho &= \rho^\dagger, \\
\sum_i p_i |i\rangle\langle i| &= \sum_i p_i |i\rangle\langle i|. \tag{2.14}
\end{aligned}$$

- ρ is positive semi-definite:

$$\begin{aligned}
\langle\psi| \left(\sum_i p_i |i\rangle\langle i|\right) |\psi\rangle &\geq 0, \\
\sum_i p_i \langle\psi|i\rangle \langle i|\psi\rangle &\geq 0, \\
\sum_i p_i |\langle\psi|i\rangle|^2 &\geq 0. \tag{2.15}
\end{aligned}$$

9

It is true because the sum of probabilities and the modulus square of inner-product will always be positive.

- Sum of diagonal elements of ρ is always equal to unity.

$$
\begin{aligned}
\text{Tr}(\rho) &= \text{Tr}\left(\sum_i p_i \, |i\rangle\langle i|\right), \\
\text{Tr}(\rho) &= \sum_i p_i \, \langle i|i\rangle, \\
\text{Tr}(\rho) &= 1.
\end{aligned}
\tag{2.16}
$$

It is also stated as the condition for valid density matrix operator.

- It is used as a tool to differentiate between pure and mixed states.

$$
\begin{aligned}
\rho^2 &= \left(\sum_i p_i \, |i\rangle\langle i|\right)\left(\sum_j p_j \, |j\rangle\langle j|\right), \\
\rho^2 &= \sum_i \sum_j p_i p_j \, |i\rangle \, \langle i|j\rangle \, \langle j|, \\
\rho^2 &= \sum_i p_i^2 \, |i\rangle\langle i|.
\end{aligned}
\tag{2.17}
$$

For the case of pure state the only possible state has probability equals to unity, thus $\rho^2 = \rho$ and $\text{Tr}(\rho^2) = \text{Tr}(\rho)$. But for mixed state the individual probability of each state is less than unity, thus its square will become a much smaller quantity resulting in $\rho^2 < \rho$ and $\text{Tr}(\rho^2) < \text{Tr}(\rho)$.

2.3.2 Bloch sphere representation

In order to write density operator in Bloch sphere representation, the state given in Eq. 2.9 is used:

$$
\begin{aligned}
\rho &= |\psi\rangle\langle\psi| \\
\rho &= \frac{1}{\sqrt{2}}\begin{bmatrix} \sqrt{1+n_z} \\ \dfrac{n_x + in_y}{\sqrt{1+n_z}} \end{bmatrix} \frac{1}{\sqrt{2}} \begin{bmatrix} \sqrt{1+n_z} & \dfrac{n_x + in_y}{\sqrt{1+n_z}} \end{bmatrix} \\
\rho &= \frac{1}{2}\begin{bmatrix} 1+n_z & n_x - in_y \\ n_x + in_y & 1 - n_z \end{bmatrix} \\
\rho &= \frac{1}{2}\left[\begin{pmatrix} 1 & 0 \\ 0 & 1 \end{pmatrix} + \begin{pmatrix} 0 & 1 \\ 1 & 0 \end{pmatrix} n_x + \begin{pmatrix} 0 & -i \\ i & 0 \end{pmatrix} n_y + \begin{pmatrix} 1 & 0 \\ 0 & -1 \end{pmatrix} n_z \right] \\
\rho &= \frac{1}{2}\left(I + \sigma_x n_x + \sigma_y n_y + \sigma_z n_z \right) \\
\rho &= \frac{1}{2}\left(I + \hat{n}.\vec{\sigma} \right) \tag{2.18}
\end{aligned}
$$

For the density operator given in Eq. 2.18 to be correct the condition for validity (Eq. 2.16) must be fulfilled. Before calculating the trace of density operator the useful identities to be known are $\mathrm{Tr}(I) = 2$, $\mathrm{Tr}(\hat{n}.\vec{\sigma}) = 0$, and $\mathrm{Tr}(\sigma_i \sigma_j) = 2\delta_{ij}$. Thus,

$$
\begin{aligned}
\mathrm{Tr}(\rho) &= \mathrm{Tr}\left[\frac{1}{2}\left(I + \hat{n}.\vec{\sigma}\right)\right] \\
\mathrm{Tr}(\rho) &= \frac{1}{2}\left[\mathrm{Tr}(I) + \mathrm{Tr}(\hat{n}.\vec{\sigma})\right] \\
\mathrm{Tr}(\rho) &= 1. \tag{2.19}
\end{aligned}
$$

To further analyze the properties of density operator in Eq.2.18, it is needed to calculate the trace of its square:

$$
\begin{aligned}
\mathrm{Tr}(\rho^2) &= \mathrm{Tr}\left[\frac{1}{2}\left(I + \hat{n}.\vec{\sigma}\right)\frac{1}{2}\left(I + \hat{n}.\vec{\sigma}\right)\right] \\
\mathrm{Tr}(\rho^2) &= \frac{1}{4}\left[\mathrm{Tr}(I^2) + 2\mathrm{Tr}(\hat{n}.\vec{\sigma}) + \mathrm{Tr}\left((\hat{n}.\vec{\sigma})(\hat{n}.\vec{\sigma})\right)\right] \\
\mathrm{Tr}(\rho^2) &= \frac{1}{4}\left[2 + \mathrm{Tr}\left((n_x\sigma_x + n_y\sigma_y + n_z\sigma_z)(n_x\sigma_x + n_y\sigma_y + n_z\sigma_z)\right)\right] \\
\mathrm{Tr}(\rho^2) &= \frac{1}{4}\left[2 + 2(n_x^2 + n_y^2 + n_z^2)\right] \\
\mathrm{Tr}(\rho^2) &= \frac{1}{2}\left[I + |n|^2\right]. \tag{2.20}
\end{aligned}
$$

11

For pure state $\text{Tr}(\rho^2) = \text{Tr}(\rho)$, which means $|n| = 1$ thus pure state lies on the boundary of Bloch sphere. In case of mixed state $\text{Tr}(\rho^2) < \text{Tr}(\rho)$, meaning $|n| < 1$ it sketches the mixed state somewhere inside the Bloch sphere. Thus, if $|n| = 0$, the state lies at the origin, such states are called the totally mixed state it gives $\text{Tr}(\rho^2) = 1/2$.

While in case of a bipartite system, the quantum state given in Eq. 2.6 the density operator follows

$$\rho_{12} = |\psi_{12}\rangle\langle\psi_{12}| . \tag{2.21}$$

In order to perform measurements on such operators, the concept of partial trace is used. It is a trace performed over subsystem such as

$$\rho_1 = \text{Tr}_2(\rho_{12}) \qquad \text{and} \qquad \rho_2 = \text{Tr}_1(\rho_{12}). \tag{2.22}$$

The partial trace has wide range of applications in quantum information and entanglement measurement.

2.4 Entangled state

For a bipartite system, a state is called an entangled state if it can not be written in the form of tensor products (unlike Eq. 2.7):

$$|\psi_{12}\rangle \neq |\psi_1\rangle \otimes |\psi_2\rangle . \tag{2.23}$$

Entanglement is the result of basis-independent superposition [41]. The mysterious behavior of entanglement collapses the measured state of one qubit into the corresponding state of other qubit.

2.4.1 Schmidt decomposition

Schmidt decomposition yields the general representation of any bipartite pure state. It states a pure state can be written as:

$$|\psi\rangle_{12} = \sum_i \sqrt{p_i} \, |i\rangle_1 \, |i'\rangle_2 . \tag{2.24}$$

Here $|i\rangle_1$ and $|i'\rangle_2$ represents the orthonormal basis of Hilbert spaces $\mathcal{H}_1$ and $\mathcal{H}_2$ respectively.

Another important term related to Schmidt decomposition is Schmidt number. It is a positive integer given by the number of coefficients of state vector associated with state $|\psi\rangle_{12}$ written in Schmidt decomposition. The Schmidt number allows us to give another mathematical definition of entanglement. It asserts that the state is entangled if Schmidt number is greater that one and the state is separable is Schmidt number is equals to unity. The simplest example of entangled state is described by Bell states.

2.4.2 Bell states

The Bell states are maximally entangled states of bipartite system. These states maximally violated the Bell inequalities. The four specific Bell states are given as:

$$
\begin{aligned}
\left|\psi^+\right\rangle_{12} &= \frac{1}{\sqrt{2}}\left[\,|0\rangle_1 \otimes |0\rangle_2 + |1\rangle_1 \otimes |1\rangle_2\,\right], \\
\left|\psi^-\right\rangle_{12} &= \frac{1}{\sqrt{2}}\left[\,|0\rangle_1 \otimes |0\rangle_2 - |1\rangle_1 \otimes |1\rangle_2\,\right], \\
\left|\phi^+\right\rangle_{12} &= \frac{1}{\sqrt{2}}\left[\,|0\rangle_1 \otimes |1\rangle_2 + |1\rangle_1 \otimes |0\rangle_2\,\right], \\
\left|\phi^-\right\rangle_{12} &= \frac{1}{\sqrt{2}}\left[\,|0\rangle_1 \otimes |1\rangle_2 - |1\rangle_1 \otimes |0\rangle_2\,\right].
\end{aligned}
\tag{2.25}
$$

The subscript $1(2)$ gives the state of qubit $1(2)$ usually called sender's (receiver's) qubit state. It can be clearly seen that the Bell states given in Eq. 2.25 are written in Schmidt decomposition. These Bell states are the linearly independent combination of two states and are also orthonormal, obeying the general conditions required for every basis set. Thus, these states made another basis set called Bell basis set, given as: $\{\left|\psi^+\right\rangle, \left|\psi^-\right\rangle, \left|\phi^+\right\rangle, \left|\phi^-\right\rangle\}$.

2.4.3 Joint operation

It is a combined operation performed on both qubits of a quantum state. Such operations generate an entanglement between two qubits. They can also change the degree of entanglement between the two already entangled qubits. For example, Hadamard

13

gate and CNOT gate combined together to form a joint operation (H+CNOT). The Hadamard gate is used to convert a qubit to superposition state. The Hadamard gate is a 2×2 matrix in a bipartite system, represented as:

$$H = \frac{1}{\sqrt{2}} \begin{bmatrix} 1 & 1 \\ 1 & -1 \end{bmatrix}. \tag{2.26}$$

The operation of Hadamard gate on states $|0\rangle$ and $|1\rangle$ respectively is given as:

$$H|0\rangle = \frac{1}{\sqrt{2}}\big(|0\rangle + |1\rangle\big), \qquad H|1\rangle = \frac{1}{\sqrt{2}}\big(|0\rangle - |1\rangle\big). \tag{2.27}$$

While CNOT gate flips the state of one qubit with respect to controlled qubit. For example, if the state of controlled qubit is 1 it will flip the state of other qubit, irrespective of its prior state. Otherwise if the state of controlled qubit is 0 the state of the other qubit remains unchanged. This joint operation (H+CNOT) is widely used for the generation and measurement of Bell states.

- **Bell state generation:** For this purpose consider the circuit given in Fig. 2.2. Suppose both the qubits are in state $|0\rangle_1$ and $|0\rangle_2$. In the first step Hadamard is applied on qubit 1. Then CNOT operation is applied on qubit 2 while controlling qubit 1. The mathematics of such circuit is given as:

$$|00\rangle_{12} \xrightarrow{H_1} \frac{1}{\sqrt{2}}\big(|0\rangle_1 + |1\rangle_1\big)|0\rangle_2 \xrightarrow{CNOT} \frac{1}{\sqrt{2}}\big(|00\rangle_{12} + |11\rangle_{12}\big) = \big|\phi^+\big\rangle. \tag{2.28}$$
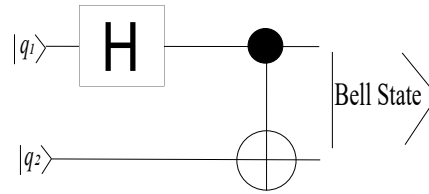
Figure 2.2: A circuit for bell state generation with initial states of first qubit ($|q_1\rangle$) and second qubit ($|q_2\rangle$).

Thus, a joint operation on un-entangled states can generate a Bell state.

14

- **Bell state measurement (BSM):** In order to measure a Bell state, the circuit given in Fig. 2.3 is used. It is a reverse of the circuit used in Bell state generation. These operation gives the result:

$$\frac{1}{\sqrt{2}}\left(|00\rangle_{12} + |11\rangle_{12}\right) \xrightarrow{CNOT} \frac{1}{\sqrt{2}}\left(|00\rangle_{12} + |10\rangle_{12}\right) \xrightarrow{H_1} |00\rangle_{12} \qquad (2.29)$$
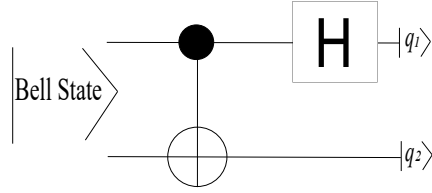
Figure 2.3: A circuit for bell state measurement resulting in state $|q_1\rangle$ of qubit 1 and $|q_2\rangle$ of qubit 2.

It gives the same prior state which was used to create a Bell state $(|\phi^+\rangle)$. Thus,it can also be proved that Hadamard and CNOT operations are unitary.

2.4.4 Local operations

The local operations are performed on a single part of two entangled qubits. Such operations does not cause entanglement nor changes the degree of entanglement. These operations include identity (I) and Pauli matrixes $(\sigma_x, \sigma_y, \sigma_z)$. In a bipartite system, these are 2×2 matrix given as:

$$I = \begin{bmatrix} 1 & 0 \\ 0 & 1 \end{bmatrix}, \quad \sigma_x = \begin{bmatrix} 0 & -1 \\ 1 & 0 \end{bmatrix}, \quad \sigma_y = \begin{bmatrix} 0 & -i \\ i & 0 \end{bmatrix}, \quad \sigma_z = \begin{bmatrix} 1 & 0 \\ 0 & -1 \end{bmatrix}. \qquad (2.30)$$

These operators are used to change an entangled state to another entangled state without disturbing its degree of entanglement.

2.5 Decoherence

Until now we studied entanglement in an isolated system, resulting in a perfect phase relation between states, called coherence. While in practical applications quantum

systems are open. It means the quantum emitters can interact with environment. The cost of this interaction is demise of coherence. For example, in order to measure entanglement quantum system has to made a contact with environment. It causes the lost of coherence that is irreversible, called decoherence. Another sight of decoherence is the lost of information related to quantum system into the environment.

2.5.1 Finite-time disentanglement

A new sight of entanglement decoherence of two qubits placed in a cavity within a finite-time was given by Yu and Eberly [31]. It is also known as early stage disentanglement or entanglement sudden death (ESD). It unfolds a wide range of investigation on finite time disentanglement under various circumstances. The main purpose of these investigation is to elude or delay ESD for advancement in quantum information technology. Though there is no way to permanently elude ESD in quantum systems but progressive work have been done to delay it such as weak and reversal measurement [42], quantum zeno effect, quantum feedback schemes [43] and many more [44, 45, 46]. While at later time another interesting phenomenon arises when the interaction between particles causes the rebirth of entanglement, called entanglement sudden birth (ESB) [47]. The time between ESD and ESB is marked with dark period of entanglement.

2.6 Entanglement measurement

It gives the numerical quantification or degree of entanglement of an entangled state. There are a number of ways to quantify entanglement such as von Neumann entropy, negativity, entanglement of formation and Wootters concurrence. In this section, a brief introduction and mathematics of von Neumann entropy and entanglement of formation is given which is followed by Wootter's concurrence.

2.6.1 von Neumann entropy

von Neumann entropy is an example of quantum entropy. In quantum communication, von Neumann entropy is used to quantify entanglement and the amount of information

retained in the system. In classical information theory, the uncertainty and randomness in the system is related to entropy. Because the information lost while sending message is a one way process, it can not be restored. While in quantum information, von Neumann entropy is used in the concept of source coding, related to the notion of information compression. It exactly gives the rate at which a quantum information source can be compressed.

Suppose a quantum system prepared in an ensemble $(\mathcal{A})$ of pure states such as: $\mathcal{A} = \{|\psi\rangle_1, |\psi\rangle_2, \cdots, |\psi\rangle_k\}$. If it is represented by density operator ρ, then von Neumann entropy is given as:

$$S(\rho) = -\text{Tr}(\rho \log_2 \rho). \tag{2.31}$$

In order to simplify this equation consider a general density operator that is diagonal in its eigen basis:

$$\rho = \begin{bmatrix} \lambda_1 & 0 & \cdots & 0 \\ 0 & \lambda_2 & \cdots & 0 \\ \vdots & \vdots & \ddots & \cdots \\ 0 & 0 & \cdots & \lambda_k \end{bmatrix},$$

$$\log_2 \rho = \begin{bmatrix} \log_2 \lambda_1 & 0 & \cdots & 0 \\ 0 & \log_2 \lambda_2 & \cdots & 0 \\ \vdots & \vdots & \ddots & \cdots \\ 0 & 0 & \cdots & \log_2 \lambda_k \end{bmatrix},$$

$$\rho \log_2 \rho = \begin{bmatrix} \lambda_1 \log_2 \lambda_1 & 0 & \cdots & 0 \\ 0 & \lambda_2 \log_2 \lambda_2 & \cdots & 0 \\ \vdots & \vdots & \ddots & \cdots \\ 0 & 0 & \cdots & \lambda_k \log_2 \lambda_k \end{bmatrix}. \tag{2.32}$$

Thus, taking trace of Eq. 2.32 gives the von Neumann entropy in terms of eigen values of the density operator:

$$-\text{Tr}\rho \log_2 \rho = -\text{Tr} \begin{bmatrix} \lambda_1 \log_2 \lambda_1 & 0 & \cdots & 0 \\ 0 & \lambda_2 \log_2 \lambda_2 & \cdots & 0 \\ \vdots & \vdots & \ddots & \cdots \\ 0 & 0 & \cdots & \lambda_k \log_2 \lambda_k \end{bmatrix},$$

$$S(\rho) = -\sum_{i=1}^{k} \lambda_i \log_2 \lambda_i. \tag{2.33}$$

17

So, $S(\rho)$ gives an average information gain per quantum state, and it only depends on the eigenvalues.

2.6.2 Entanglement of formation and Wootters concurrence

One of the most important method of measuring entanglement in bipartite system is the entanglement of formation brought forward by Bennett *et. al.* [48]. It is given as

$$E(\rho) = min \sum_i p_i S(\rho), \tag{2.34}$$

here $E(\rho)$ is the entanglement of formation giving the average entanglement of all possible values of pure state. Whereas, $S(\rho)$ is the von Neumann entropy of either of the two system, given as

$$S(\rho) = -\text{Tr}(\rho_1 \log_2 \rho_1) = -\text{Tr}(\rho_2 \log_2 \rho_2). \tag{2.35}$$

This formalism is widely expected for the pure state of bipartite system. While in order to measure the entanglement of a mixed state, which is a linear combination of pure states Eq. 2.34 doesn't remain valid. In order to tackle this issue, Wootters and Hill [49] extented the idea of Bennett *et. al.* and gives an explicit formula of concurrence depending on density operator elements. The numerical value of concurrence varies between zero and one. Concurrence is zero if the state is separable and is equal to one for maximally entangled state. Thus the entanglement of formation in the form of binary entropy is given as [50]

$$E(\rho) = -\lambda_+ \log_2 \lambda_+ - \lambda_- \log_2 \lambda_-, \tag{2.36}$$

where

$$\lambda_\pm = \frac{1 \pm \sqrt{1 - C(\rho)^2}}{2} \tag{2.37}$$

Here $C(\rho)$ is called concurrence which is given as [49]:

$$C(\rho) = 2max\{0, \sqrt{\zeta_1} - \sqrt{\zeta_2} - \sqrt{\zeta_3} - \sqrt{\zeta_4}\}, \tag{2.38}$$

where the $\zeta's$ are the eigenvalues of hermitian matrix $M(\rho) = \sqrt{\rho}\tilde{\rho}\sqrt{\rho}$ in descending order. Here $\tilde{\rho} = (\sigma_y \otimes \sigma_y)\rho^*(\sigma_y \otimes \sigma_y)$, with σ_y a Pauli operator and ρ^* being conjugate of

operator ρ. While the discussion involved in this dissertation is marked with X-states [51]. These are the states having only diagonal and anti-diagonal elements of density operator, forming an X-structure such as [52]:

$$\rho = \begin{bmatrix} \rho_{11} & 0 & 0 & \rho_{14} \\ 0 & \rho_{22} & \rho_{23} & 0 \\ 0 & \rho_{23}^* & \rho_{33} & 0 \\ \rho_{14}^* & 0 & 0 & \rho_{44} \end{bmatrix}. \tag{2.39}$$

This group of states include Bell states, Werner state, maximally non-local mixed state (MNMS) and maximally entangled mixed state (MEMS). The main motivation behind studying X-states is their property of invariance with time evolution. For the density operator given in Eq. 2.39, the concurrence simply takes the form

$$C(t) = 2max[0, C_1(t), C_2(t)], \tag{2.40}$$

where

$$C_1(t) = |\rho_{23}(t)| - \sqrt{\rho_{11}(t)\rho_{44}(t)} , \qquad C_2(t) = |\rho_{14}(t)| - \sqrt{\rho_{22}(t)\rho_{33}(t)}. \tag{2.41}$$

It is the definition of concurrence given in decoupled basis (see Eq. 2.7), which depends on the elements of density operator.

2.7 Entanglement applications

Entanglement is used as a resource in many practical applications such as quantum communication, quantum computing and quantum sensing. The astonishing applications of quantum communication are cryptography, superdense coding, entanglement swapping and quantum teleportation. The field of cryptography applies the basis concept of quantum superposition which gives more secure way to communicate between two parties (Alice and Bob). Entanglement swapping enables us to induce entanglement between two independent qubits that never interacted before. Quantum teleportation is a technique used to communicate information between sender (Alice) and receiver (Bob) without physically sending qubits or particles. Another remarkable application

19

of quantum communication is superdense coding (SDC), which enhances the classical communication by physically sending a qubit that encapsulated the information two classical bits. The detailed protocol and basics of SDC are explained in the following.

2.7.1 Superdense coding

SDC was first discovered by Bennette and Wisner using an EPR pair. Suppose Alice and Bob shared an entangled pair prepared initially in Bell state "$\left|\phi^+\right\rangle_{12}$". The protocol for superdense coding works as follows:

- **Step 1:** In the very first step, Alice will decide a coding of each possible state for a given number of bits.

- **Step 2:** Alice will perform local unitary operations $(I, \sigma_x, \sigma_y, \sigma_z)$ on her qubit. This is done to convert the initial state of EPR pair to the state she wants to communicate to Bob.

- **Step 3:** Now, its time for Alice to send her qubit physically through quantum channel to Bob.

- **Step 4:** Bob will performs a joint operation (BSM) on both qubits to extract the conveyed information.
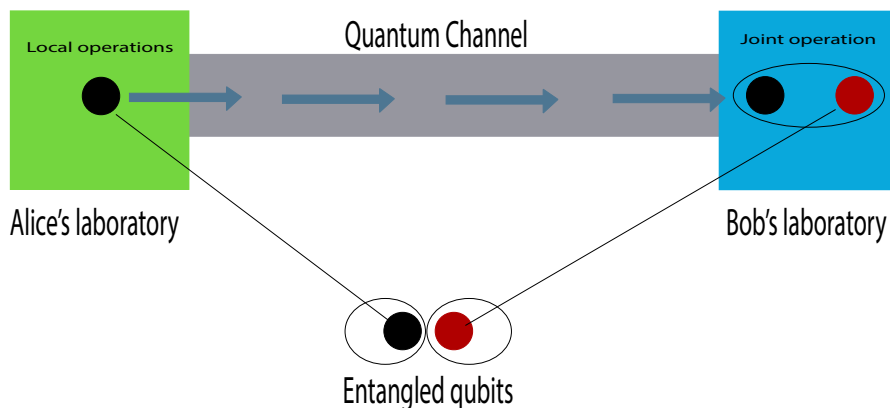

Figure 2.4: A schematic protocol for superdense coding of two entangled particles initially in state $\left|\phi^+\right\rangle_{12}$ shared between Alice and Bob.

Step 1		Step 2	Step 3	Step 4
Alice wants to communicate the state	Coding	Local operations on Alice's qubit	Bob received the state	Result of BSM performed by Bob
$\lvert 00 \rangle$	$\lvert \phi^+ \rangle_{12}$	$\lvert \phi^+ \rangle_{12} \xrightarrow{I^1 \otimes I^2} \lvert \phi^+ \rangle_{12}$	$\lvert \phi^+ \rangle_{12}$	$\lvert 00 \rangle$
$\lvert 01 \rangle$	$\lvert \psi^+ \rangle_{12}$	$\lvert \phi^+ \rangle_{12} \xrightarrow{\sigma_x^1 \otimes I^2} \lvert \psi^+ \rangle_{12}$	$\lvert \psi^+ \rangle_{12}$	$\lvert 01 \rangle$
$\lvert 10 \rangle$	$\lvert \phi^- \rangle_{12}$	$\lvert \phi^+ \rangle_{12} \xrightarrow{\sigma_z^1 \otimes I^2} \lvert \phi^- \rangle_{12}$	$\lvert \phi^- \rangle_{12}$	$\lvert 10 \rangle$
$\lvert 11 \rangle$	$\lvert \psi^- \rangle_{12}$	$\lvert \phi^+ \rangle_{12} \xrightarrow{\sigma_y^1 \otimes I^2} \lvert \psi^- \rangle_{12}$	$\lvert \psi^- \rangle_{12}$	$\lvert 11 \rangle$

Table 2.1: Protocol for superdense coding

Holevo information ($\chi(\epsilon)$): Holevo information sets an upper bound on the dense coding capacity. It gives the numerical value of maximum compression of information a qubit can contain. The von Neumann entropy (Sec. 2.62) also quantifies the amount of information compressed, but Eq. 2.33 is applicable to an ensemble of pure states. Suppose the quantum system is prepared in an ensemble ($\mathcal{B}$) of mixed states such that: $\mathcal{B} = \{\rho_1, \rho_2, \cdots, \rho_k\}$. For this case Eq. 2.31, can be written as:

$$
\begin{aligned}
S(\rho) &= -\mathrm{Tr}\rho \log_2 \rho, \\
S(\rho) &= -\mathrm{Tr}\left[\sum_i p_i \rho_i \log_2 \left[\sum_i p_i \rho_i \right] \right], \\
S(\rho) &= -\sum_i \mathrm{Tr}\left[p_i \rho_i \left[\log_2 p_i + \log_2 \rho_i \right] \right], \\
S(\rho) &= -\sum_i p_i \log_2 p_i - \sum_i p_i \mathrm{Tr}\rho_i \log_2 \rho_i, \\
S(\rho) &= H(p_1, \cdots, p_k) + \sum_i p_i S(\rho_i).
\end{aligned} \tag{2.42}
$$

Where $H(p_1, \cdots, p_k)$ is classical entropy also known as Shannon entropy, it gives date compression in classical channel. Here we introduced a new quantity $\chi(\epsilon)$ where $\epsilon =$

$\{p_1, \cdots, p_k, \rho_1, \cdots, \rho_k\}$, such that:

- $\chi(\epsilon) = H(p)$ for mutually orthonogal mixed states.

- $\chi(\epsilon) = S(\rho)$ for an ensemble of pure states.

- $\chi(\epsilon) = 0$ for only one mixed state.

To fulfill this description the quantity $\chi(\epsilon)$ known as Holevo information is given as:

$$\chi(\epsilon) = S(\rho) - \sum_i p_i S(\rho_i). \tag{2.43}$$

The quantity $\chi(\epsilon)$ gives us an average capacity of a qubit, that how much classical information can be conveyed through one qubit.

Chapter 3

Entanglement Creation - A Review

This chapter is marked with the discussion of the concept of creating steady entanglement out of thermal equilibrium. For this purpose, in Sec. 3.1 the brief introduction of interaction between atom and field is given which is supported by the discussion of interaction with thermal fields. Then in Sec. 3.2 we described the theoretical model of two quantum emitters placed close to a thermal body, held at different temperatures from its surroundings. Lastly, in Sec. 3.3 the implementation of the model dynamics for achieving steady state entanglement is explained.

3.1 Atom-field interaction

It is the interaction between a two-level atom treated as a quantum system and a single-mode electric field. While an atom-field interaction could be of two types, such as interaction with a classical electric field called *atom-field interaction semi-classical theory* or with a quantized electric field called *atom-field interaction quantum theory*. The prior one is valid for many assumptions such as in describing the method of measurement using time delay spectroscopy and the phenomena of stimulated emission and absorption in laser and maser. However, there are many phenomenons where semi-classical theory fails, one of the most important of these is the occurrence of spontaneous emission. Thus, for explaining such phenomenons we need the quantum explanation of atom-field interaction. To this aim, the fully quantum model also called

Jaynes–Cummings model is discussed further which has no analog in semi-classical theory.

3.1.1 Jaynes-Cummings model

This model was fist established by Edwin Jaynes and Fred Cummings in their 1963 article. It was intended to illuminate the concept of fully quantum model to treat the interaction of atom with single-mode electromagnetic (EM) field. Consider a two-level quantum system with a ground state $|g\rangle$ and an excited state $|e\rangle$ which is interacting with the single-mode quantized EM field. Thus, in an open quantum system the total Hamiltonian (H) is the sum of atomic Hamiltonian (H_A), the Hamiltonian of the environment (H_E) and the interaction Hamiltonian (H_I) between atom and its environment given as

$$\begin{aligned} H &= H_A + H_E + H_I, \\ H &= \left[\frac{p^2}{2m} + V(r)\right] + \left[\frac{1}{2}(p^2 + \omega^2 q^2)\right] + \left[-D.E\right], \end{aligned} \tag{3.1}$$

where (H_A) is simply given as the total energy (kinetic energy + potential energy). While (H_E) is as classical field Hamiltonian also called environmental Hamiltonian, where p and q are the canonical variables called position (q) and momentum (p). The (H_I) is given by the concept of perturbation theory, where D is the dipole moment and E is the EM field. In order to write Eq. 3.1 in fully quantum model we need to write them in the form of quantized operators. Let these operators are atomic operators called raising (σ_{eg}) and lowering (σ_{ge}) operator, and field operators called $a(a^\dagger)$ annihilation and creation operator given as

$$\sigma_{eg} = |e\rangle\langle g|, \qquad \sigma_{ge} = |g\rangle\langle e|, \tag{3.2}$$

and

$$a = \frac{\omega q + ip}{\sqrt{2\hbar\omega}}, \qquad a^\dagger = \frac{\omega q - ip}{\sqrt{2\hbar\omega}}. \tag{3.3}$$

Now we will use these operators to rewrite Eq. 3.1 in fully quantum model. Atomic Hamiltonian (H_A) in the form of operators can also be written as

$$
\begin{aligned}
H_A &= \Big[\sum_i |i\rangle\langle i|\Big] H_A \Big[\sum_j |j\rangle\langle j|\Big], \\
H_A &= \sum_{ij} \hbar\omega_j |i\rangle \langle i|j\rangle \langle j|, \\
H_A &= \sum_i \hbar\omega_i |i\rangle\langle i|, \\
H_A &= \hbar\omega_g |g\rangle\langle g| + \hbar\omega_e |e\rangle\langle e|.
\end{aligned}
\tag{3.4}
$$

Using operators given in Eq. 3.2, we can write

$$
\begin{aligned}
H_A &= E_g \sigma_{ge}\sigma_{eg} + E_e \sigma_{eg}\sigma_{ge}, \\
H_A &= \frac{1}{2} E_g \sigma_{ge}\sigma_{eg} + \frac{1}{2} E_g \sigma_{ge}\sigma_{eg} + \frac{1}{2} E_e \sigma_{eg}\sigma_{ge} + \frac{1}{2} E_e \sigma_{eg}\sigma_{ge}.
\end{aligned}
\tag{3.5}
$$

After adding and subtracting $\frac{1}{2} E_g \sigma_{ge}\sigma_{eg}$ and $\frac{1}{2} E_e \sigma_{eg}\sigma_{ge}$, we get

$$
H_A = \frac{1}{2}\left(E_e + E_g\right)\left[\sigma_{eg}\sigma_{ge} + \sigma_{ge}\sigma_{eg}\right] + \frac{1}{2}\left(E_e - E_g\right)\left[\sigma_{eg}\sigma_{ge} - \sigma_{ge}\sigma_{eg}\right].
\tag{3.6}
$$

Here the first term can be ignored under the rotating wave approximation.

$$
H_A = \frac{1}{2}\hbar\omega_0 \sigma_z,
\tag{3.7}
$$

where $\hbar\omega_0$ is the difference between two-energy levels and σ_z is the Pauli operator. In order to quantize environmental Hamiltonian Eq. 3.3 can be rewritten as

$$
p = -i\sqrt{\frac{\hbar\omega}{2}}\left(a - a^\dagger\right), \qquad\qquad q = \sqrt{\frac{\hbar}{2\omega}}\left(a + a^\dagger\right).
\tag{3.8}
$$

Thus,

$$
\begin{aligned}
H_E &= \frac{1}{2}\left(\left(-\frac{\hbar\omega}{2}(a - a^\dagger)^2\right) + \omega^2\left(\frac{\hbar}{2\omega}(a + a^\dagger)^2\right)\right), \\
H_E &= \frac{\hbar\omega}{4}\left(-a^2 - a^{\dagger 2} + aa^\dagger + a^\dagger a + a^2 + a^{\dagger 2} + aa^\dagger + a^\dagger a\right), \\
H_E &= \frac{\hbar\omega}{2}\left(aa^\dagger + a^\dagger a\right).
\end{aligned}
\tag{3.9}
$$

By using the property $[a, a^\dagger] = 1$, we can write

$$H_E = \hbar\omega\left(aa^\dagger + 1/2\right). \qquad (3.10)$$

It is the quantized environmental Hamiltonian. Now in order to write interaction Hamiltonian in quantum operators we need quantized electric field given as

$$\hat{E} = -j\zeta(a + a^\dagger), \qquad (3.11)$$

where j is the electric field polarization vector and ζ is given as

$$\zeta = -\left(\frac{\hbar\omega}{\epsilon_o U}\right)^{1/2} sin(kx). \qquad (3.12)$$

So, the interaction Hamiltonian becomes

$$H_I = \hat{d}\zeta(a + a^\dagger), \qquad (3.13)$$

where $\hat{d} = D.j$ and due to parity conditions only the diagonal elements of this dipole operator will be non-zero. Thus,

$$\hat{d} = d_{gg}\,|g\rangle\langle g| + d_{ge}\,|g\rangle\langle e| + d_{eg}\,|e\rangle\langle g| + d_{ee}\,|e\rangle\langle e|,$$
$$\hat{d} = d_{ge}\,|g\rangle\langle e| + d_{eg}\,|e\rangle\langle g|. \qquad (3.14)$$

For simplicity we assume that the coefficient d is real such as $d_{eg} = d_{eg}^* = d$ and rewriting above equation in field operators (Eq. 3.3) form

$$\hat{d} = d(\sigma_{ge} + \sigma_{eg}). \qquad (3.15)$$

So,

$$H_I = d(\sigma_{ge} + \sigma_{eg})\zeta(a + a^\dagger),$$
$$H_I = d\zeta(\sigma_{ge}a + \sigma_{ge}a^\dagger + \sigma_{eg}a + \sigma_{eg}a^\dagger). \qquad (3.16)$$

Here the operators a, $a^\dagger$, σ_{ge} and σ_{eg} evolves with time, thus we use the Heisenberg picture to write these operators as

$$a(t) = a(0)e^{-i\omega t}, \qquad a^\dagger(t) = a(0)^\dagger e^{i\omega t}. \qquad (3.17)$$

26

and

$$\sigma_{ge}(t) = \sigma_{ge}(0)e^{-i\omega_0 t}, \qquad \sigma_{eg}(t) = \sigma_{eg}(0)e^{i\omega_0 t}. \tag{3.18}$$

Thus,

$$H_I = d\zeta(\sigma_{ge}ae^{-i(\omega+\omega_0)t} + \sigma_{ge}a^\dagger e^{i(\omega-\omega_0)t} + \sigma_{eg}ae^{-i(\omega-\omega_0)t} + \sigma_{eg}a^\dagger e^{i(\omega+\omega_0)t}). \tag{3.19}$$

Here the first and last term will be neglected under to rotating wave approximation and for simplicity we assume $\omega \approx \omega_0$ so,

$$H_I = d\zeta(\sigma_{ge}a^\dagger + \sigma_{eg}a). \tag{3.20}$$

Now putting Eqs. 3.7, 3.10 and 3.20 in Eq. 3.1, we get

$$H = \frac{1}{2}\hbar\omega\sigma_z + \hbar\omega\big(aa^\dagger + 1/2\big) + d\zeta\big(\sigma_{ge}a^\dagger + \sigma_{eg}a\big). \tag{3.21}$$

This is called the Jaynes Cummings Hamiltonian given in fully quantum model for a single two-level system.

3.1.2 Thermal fields

Consider the environment of a quantum system is a thermal reservoir for example a perfect absorber and emitter called a black-body. This black-body can be designed as a cavity whose walls are present at thermal equilibrium with the radiations. These radiations then coupled to a heat bath. Here, assume the coupling between them is weak, so that we can describe the system as micro-canonical ensemble which gives the probability of particle in nth excited state as

$$p_n = \frac{\exp(-\beta E_n)}{\sum_{n=0}^{\infty}\exp(-\beta E_n)} = \frac{\exp(-\beta E_n)}{Z}, \tag{3.22}$$

where $\beta = k_B/T$ with k_B as boltzmann constant and T is the temperature of the cavity, E_n is the energy of nth state and Z is the partition function of micro-canonical ensemble. With $E_n = \hbar\omega(n + 1/2)$, we can rewrite Z as follows

$$Z = \exp(-\beta\hbar\omega/2)\sum_{n=0}^{\infty}\exp(-\beta\hbar\omega n E_n) = \frac{\exp(-\beta\hbar\omega/2)}{1 - \exp(-\beta\hbar\omega)}. \tag{3.23}$$

Similarly,

$$p_n = \frac{\exp\left(-\beta\hbar\omega(n+1/2)\right)}{Z}. \tag{3.24}$$

Now in order to write Eqs. 3.23, 3.24 in terms of average photon number $\bar{n}(\omega, T)$ of thermal field, we will define $\bar{n}(\omega, T)$ as

$$
\begin{aligned}
\bar{n}(\omega, T) &= \sum_{n=0}^{\infty} n p_n, \\
\bar{n}(\omega, T) &= \frac{\exp(-\beta\hbar\omega/2)}{Z} \sum_{n=0}^{\infty} n\exp(-\beta\hbar\omega n), \\
\bar{n}(\omega, T) &= \frac{1}{\exp(\beta\hbar\omega) - 1}.
\end{aligned} \tag{3.25}
$$

It gives us $\exp(-\beta\hbar\omega) = \bar{n}(\omega, T)/\left(1 + \bar{n}(\omega, T)\right)$ so that we can write

$$
\begin{aligned}
Z &= \frac{\exp(-\beta\hbar\omega)1/2}{1 - \exp(-\beta\hbar\omega)}, \\
Z &= \frac{\left[\bar{n}(\omega, T)/\left(1 + \bar{n}(\omega, T)\right)\right]^{1/2}}{1 - \left[\bar{n}(\omega, T)/\left(1 + \bar{n}(\omega, T)\right)\right]}, \\
Z &= \left[\bar{n}(\omega, T)\left(1 + \bar{n}(\omega, T)\right)\right]^{1/2}.
\end{aligned} \tag{3.26}
$$

Similarly,

$$
\begin{aligned}
p_n &= \frac{\left[\exp(-\beta\hbar\omega)1/2\right]\left[\exp(-\beta\hbar\omega)n\right]}{Z}, \\
p_n &= \frac{\left[\bar{n}(\omega, T)/\left(1 + \bar{n}(\omega, T)\right)\right]^{1/2}\left[\bar{n}(\omega, T)/\left(1 + \bar{n}(\omega, T)\right)\right]^{n}}{\left[\bar{n}(\omega, T)\left(1 + \bar{n}(\omega, T)\right)\right]^{1/2}}, \\
p_n &= \frac{\left(\bar{n}(\omega, T)\right)^{n}}{\left(1 + \bar{n}(\omega, T)\right)^{1/2}}.
\end{aligned} \tag{3.27}
$$

Thus, the thermal density operator can be obtained by using the definition of density operator (see Eq. 2.11)

$$
\begin{aligned}
\rho_{th} &= \sum_{n=0}^{\infty} p_n \left|n\right\rangle\!\left\langle n\right|, \\
\rho_{th} &= \frac{1}{1 + \left(\bar{n}(\omega, T)\right)} \sum_{n=0}^{\infty} \left(\frac{\left(\bar{n}(\omega, T)\right)}{1 + \left(\bar{n}(\omega, T)\right)}\right)^{n} \left|n\right\rangle\!\left\langle n\right|.
\end{aligned} \tag{3.28}
$$

It is a relation for thermal density operator at thermal equilibrium between qubit and walls of the cavity.

3.2 The model

Consider two quantum emitters (qubits), whose excited and ground levels are separated by frequency ω. These quantum emitters are placed close to an arbitrary body (A) having particular dielectric constant and kept at temperature T_A, surrounded by a far away boundary (B) having temperature T_B. The arbitrary body and boundary are kept at different but constant temperatures that produces stationary and out-of-thermal equilibrium Electromagnetic (EM) fields. The total Hamiltonian (H) of the system is the sum of the qubit's Hamiltonian, the Hamiltonian of the thermal bath, and the interaction Hamiltonian:

$$
\begin{aligned}
H &= H_q + H_b + H_{int}, \\
&= \sum_q \sum_{i=g,e} \hbar \omega_i^q \sigma_{ii}^q + \sum_j \epsilon_j \hat{a}_j^\dagger \hat{a}_j - \sum_q D_q \cdot E(r_q),
\end{aligned}
\tag{3.29}
$$

being $\sigma_{ii}^q = |i\rangle_{qq} \langle i|$ where g and e are the ground and excited levels of qubits respectively. The ϵ_j in environmental Hamiltonian is Bogoliubov spectrum, whereas $\hat{a}^\dagger$ and $\hat{a}$ are the raising and lowering operators respectively. The term D_q in interaction Hamiltonian is the electric-dipole multipolar coupling operator and $E(r_q)$ is the electric field of qubit at position r_q from the body.
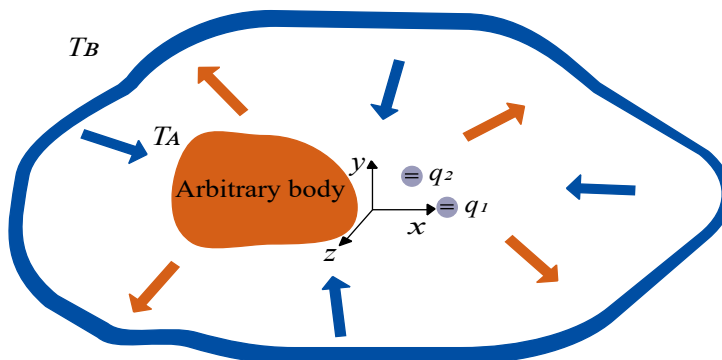

Figure 3.1: A schematic diagram of two qubits (q_1 and q_2) placed closed to an arbitrary body kept at temperature T_A and the surrounding boundary has a constant temperature T_B such that $T_A \neq T_B$.

3.2.1 Master equation

It is the equation that gives the time evolution of open quantum systems. The equations deduced from Master equation are called rate equations. The dynamics of a two-level system is studied by employing the master equation approach explained in Ref. [53],

$$
\begin{aligned}
\frac{d\rho(t)}{dt} &= -\frac{i}{\hbar}[H_q, \rho] - i\sum_{q \neq q'} \Lambda^{qq'}(\omega)[\sigma^q_{eg}\sigma^{q'}_{ge}, \rho] \\
&+ \sum_{qq'} \Gamma^{qq'}(\omega)\left(\sigma^{q'}_{ge}\rho\sigma^q_{eg} - \frac{1}{2}\{\sigma^q_{eg}\sigma^{q'}_{ge}, \rho\}\right) \\
&+ \sum_{qq'} \Gamma^{qq'}(-\omega)\left(\sigma^{q'}_{eg}\rho\sigma^q_{ge} - \frac{1}{2}\{\sigma^q_{ge}\sigma^{q'}_{eg}, \rho\}\right).
\end{aligned}
\tag{3.30}
$$

The term $\Lambda^{qq'}(\omega)$ represents dipole-dipole interaction independent of temperature. Contrarily, term $\Gamma^{qq'}(\pm\omega)$ gives transition rates depending on both thermal and quantum fluctuations of EM fields, being $q = q'$ depicts individual and $q \neq q'$ illustrates collective transition rates. For the quantum state out of thermal equilibrium, these transition rates take the form [54],

$$
\begin{aligned}
\Gamma^{qq'}(\omega) &= \sqrt{\Gamma^q_0(\omega)\Gamma^{q'}_0(\omega)}\{[1 + n(\omega, T_A)]\eta^{qq'}_A(\omega) \\
&\quad + [1 + n(\omega, T_B)]\eta^{qq'}_B(\omega)\}, \\
\Gamma^{qq'}(-\omega) &= \sqrt{\Gamma^q_0(\omega)\Gamma^{q'}_0(\omega)}\{n(\omega, T_A)\eta^{qq'}_A(\omega)^* \\
&\quad + n(\omega, T_B)\eta^{qq'}_B(\omega)^*\}.
\end{aligned}
\tag{3.31}
$$

Where $\eta^{qq'}_A(\omega)$ and $\eta^{qq'}_B(\omega)$ are functions dependent on transmission and reflection scattering rates and other parameters of the system briefly explained in Ref. [54].

3.2.2 Density matrix elements

In order to inspect our approach to a quantum system out of thermal equilibrium we considered Dicke bases [55],

$$
|G\rangle = |0\rangle, |S\rangle = \frac{(|1\rangle + |2\rangle)}{\sqrt{2}}, |A\rangle = \frac{(|1\rangle - |2\rangle)}{\sqrt{2}}, |E\rangle = |3\rangle.
\tag{3.32}
$$

Here $|G\rangle$ and $|E\rangle$ are excited and ground states, whereas $|S\rangle$ and $|A\rangle$ are symmetric and anti-symmetric states. Whereas, $|0\rangle = |00\rangle$, $|1\rangle = |01\rangle$, $|2\rangle = |10\rangle$ and $|3\rangle = |11\rangle$ (Eq. 2.7). The schematic diagram for Dicke basis is given in Fig. 3.2.
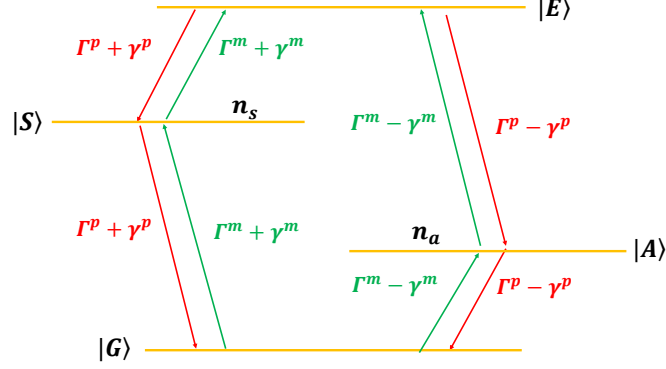

Figure 3.2: Schematic representation of coupled basis, here $\Gamma^p = \Gamma(\omega)$, $\Gamma^m = \Gamma(-\omega)$, $\gamma^p = \gamma(\omega)$ and $\gamma^m = \gamma(-\omega)$.

The master equation (Eq. 3.30) when analyzed in the coupled bases (Dicke basis), gives only the diagonal and anti-diagonal density matrix elements forming an X-structure. In our case, these diagonal and anti-diagonal terms are invariant under time evolution [54]. Therefore, the density matrix elements for a quantum system out of thermal equilibrium ($T_A \neq T_B$) will be given as

$$
\begin{aligned}
\dot{\rho}_{GG} &= \Gamma_a(1+n_a)\rho_{AA} + \Gamma_s(1+n_s)\rho_{SS} \\
&\quad -(\Gamma_a n_a + \Gamma_s n_s)\rho_{GG}, \\
\dot{\rho}_{AA} &= \Gamma_a n_a \rho_{GG} + \Gamma_a(1+n_a)\rho_{EE} - \Gamma_a(1+2n_a)\rho_{AA}, \\
\dot{\rho}_{SS} &= \Gamma_s n_s \rho_{GG} + \Gamma_s(1+n_s)\rho_{EE} - \Gamma_s(1+2n_s)\rho_{SS}, \\
\dot{\rho}_{EE} &= \Gamma_a n_a \rho_{AA} + \Gamma_s n_s \rho_{SS} \\
&\quad -[\Gamma_a(1+2n_a) + \Gamma_s(1+2n_s)]\rho_{EE}, \\
\dot{\rho}_{AS} &= \frac{1}{2}[4i\Lambda^{12}(\omega) - \Gamma_a(1+2n_a) - \Gamma_s(1+2n_s)]\rho_{AS}, \\
\dot{\rho}_{GE} &= \frac{1}{2}[4i\Lambda^{12}(\omega) - \Gamma_a(1+2n_a) - \Gamma_s(1+2n_s)]\rho_{GE},
\end{aligned}
$$

$$(3.33)$$

31

with $\dot{\rho}_{SA} = \dot{\rho}_{AS}^*$, and $\dot{\rho}_{EG} = \dot{\rho}_{GE}^*$. The expressions Γ_a and Γ_s in Eq. (3.33) are obtained by following the strategy employed in Ref. [53],

$$\Gamma(\omega) + \gamma(\omega) = \Gamma_0(\omega)\Gamma_a(1 + n_a),$$
$$\Gamma(\omega) + \gamma(\omega) = \Gamma_0(\omega)\Gamma_s(1 + n_s),$$
$$\Gamma(-\omega) - \gamma(-\omega) = \Gamma_0(\omega)\Gamma_s n_a,$$
$$\Gamma(-\omega) - \gamma(-\omega) = \Gamma_0(\omega)\Gamma_s n_s. \tag{3.34}$$

Here $\Gamma^{11}(\pm\omega) = \Gamma^{22}(\pm\omega) = \Gamma(\pm\omega)$ and $\Gamma^{21}(\pm\omega) = \Gamma^{12}(\pm\omega) = \gamma(\pm\omega)$. In order to normalize Eq. (3.34) with time, the coefficient $\Gamma_0(\omega)$ is consumed within the time derivative. The terms Γ_s and Γ_a are the transition rates of super- and sub-radiant states respectively, whereas n_s and n_a give the effective number of photons in individual super and sub-radiant levels at temperatures T_s and T_a in between T_A and T_B.

$$
\begin{aligned}
\Gamma_a &= \eta_B(\omega) - \eta_B^{12}(\omega) + \eta_A(\omega) - \eta_A^{12}(\omega) \tag{3.35}\\
\Gamma_s &= \eta_B(\omega) + \eta_B^{12}(\omega) + \eta_A(\omega) + \eta_A^{12}(\omega)\\
n_a &= \frac{1}{\Gamma_a}\{[\eta_B(\omega) - \eta_B^{12}(\omega)]n(\omega, T_B)\\
&\quad + [\eta_A(\omega) - \eta_A^{12}(\omega)]n(\omega, T_A)\}\\
n_s &= \frac{1}{\Gamma_s}\{[\eta_B(\omega) + \eta_B^{12}(\omega)]n(\omega, T_B)\\
&\quad + [\eta_A(\omega) + \eta_A^{12}(\omega)]n(\omega, T_A)\}
\end{aligned}
$$

In the next section, the investigation of steady entanglement is done for both at equilibrium and out of thermal equilibrium cases.

3.3   Steady entanglement

Generally, a steady state is a state or a condition that is invariant in time. While in quantum systems this regime can play an important role in giving rise to particular phenomena known as steady state entanglement. In this section we study this phenomena first for the quantum system at thermal equilibrium and then at out of thermal equilibrium.

3.3.1 At thermal equilibrium

At thermal equilibrium $(T_A = T_B)$, the density operator stated in equation Eq. 3.28 gives only diagonal elements. Thus, the master equation describes the steady diagonal elements as

$$\begin{pmatrix} \rho_{11}(\infty) \\ \rho_{22}(\infty) \\ \rho_{33}(\infty) \\ \rho_{44}(\infty) \end{pmatrix} = \frac{1}{Z} \begin{pmatrix} \left(1 + n(\omega, T)\right)^2 \\ 1 + n(\omega, T)\left(1 + n(\omega, T)\right) \\ 1 + n(\omega, T)\left(1 + n(\omega, T)\right) \\ n(\omega, T) \end{pmatrix} \tag{3.36}$$

Now using the definition of concurrence expressed in Eq. 2.41 it can be seen that $C_1 < 0$ also $C_2 < 0$ resulting in non-entangled steady states at thermal equilibrium.

3.3.2 Out of thermal equilibrium

With a view to study steady state entanglement out of thermal equilibrium we used Dicke basis (see Eq. 3.32). To this aim we also have to rewrite concurrence (Eq. 2.41) in such basis.

$$\begin{aligned} C(t) &= 2max\{0, C_1(t), C_2(t)\}, \\ C_1(t) &= |\rho_{EG}(t)| \\ &\quad - \frac{1}{2}\sqrt{(\rho_{SS}(t) + \rho_{AA}(t))^2 - (\rho_{SA}(t) + \rho_{AS}(t))^2}, \\ C_2(t) &= \frac{1}{2}\sqrt{(\rho_{SS}(t) - \rho_{AA}(t))^2 - (\rho_{SA}(t) - \rho_{AS}(t))^2} \\ &\quad - \sqrt{\rho_{EE}(t)\rho_{GG}(t)}. \end{aligned} \tag{3.37}$$

The result of Eq. 3.33 at steady state gives only diagonal elements:

$$\begin{pmatrix} \rho_{GG}(\infty) \\ \rho_{AA}(\infty) \\ \rho_{SS}(\infty) \\ \rho_{EE}(\infty) \end{pmatrix} = \frac{1}{Z_{eq}} \begin{pmatrix} (1 + n_a)^2(1 + 2n_s)\Gamma_a + (1 + 2n_a)(1 + n_s)^2\Gamma_s \\ n_a(1 + n_a)(1 + 2n_s)\Gamma_a + \left[n_a(1 + 2n_s) + n_s^2(1 + 2n_a)\right]\Gamma_s \\ n_s(1 + n_s)(1 + 2n_a)\Gamma_s + \left[n_s(1 + 2n_a) + n_a^2(1 + 2n_s)\right]\Gamma_a \\ n_a^2(1 + 2n_s)\Gamma_a + (1 + 2n_a)n_s^2\Gamma_s \end{pmatrix}, \tag{3.38}$$

where Z_{eq} is the sum of all the elements on the right side of the above equation. It can be discern from Eq. 3.37 that $C_1 < 0$ so it will not play any role in steady state entanglement. While C_2 at steady state becomes

$$C_2(\infty) = \frac{1}{2Z_{eq}}\sqrt{[\rho_{SS}(\infty) - \rho_{AA}(\infty)]^2} - \sqrt{\rho_{GG}(\infty)\rho_{EE}(\infty)}. \tag{3.39}$$

33

where

$$\rho_{SS}(\infty) - \rho_{AA}(\infty) = \left(n_s(1+n_s)(1+2n_a)\Gamma_s + \left[n_S(1+2n_a) + n_a^2(1+2n_s)\right]\Gamma_a\right)$$
$$-\left(n_a(1+n_a)(1+2n_s)\Gamma_a - \left[n_a(1+2n_s) + n_s^2(1+2n_a)\right]\Gamma_s\right),$$

$$\rho_{SS}(\infty) - \rho_{AA}(\infty) = \left((n_s(1+n_s)(1+2n_a) - n_a(1+2n_s) - n_s^2(1+2n_a)\right)\Gamma_s$$
$$+\left(n_s(1+2n_a) + n_a^2(1+2n_s) - (n_a(1+n_a)(1+n_s)\right)\Gamma_a,$$

$$\rho_{SS}(\infty) - \rho_{AA}(\infty) = \left(n_s + n_s^2(1+2n_a) - n_a - 2n_s n_a - n_s^2 - 2n_a n_s^2\right)\Gamma_s$$
$$+\left(n_s + 2n_s n_a + n_a^2 + 2n_a^2 n_s - \left((n_a + n_a^2)(1+2n_s)\right)\right)\Gamma_a,$$

$$\rho_{SS}(\infty) - \rho_{AA}(\infty) = \left(n_s + n_s^2 + 2n_a n_s^2 - n_a - 2n_s n_a - n_s^2 - 2n_a n_s^2\right)\Gamma_s$$
$$+\left(n_s + 2n_s n_a + n_a^2 + 2n_a^2 n_s - n_a - n_a^2 - 2n_a n_s - 2n_a^2 n_s\right)\Gamma_a,$$

$$\rho_{SS}(\infty) - \rho_{AA}(\infty) = (n_s - n_a)(\Gamma_s + \Gamma_a). \tag{3.40}$$

Hence,

$$C_2(\infty) = \frac{1}{2Z_{eq}} \left[\sqrt{(|n_s - n_a|(\Gamma_s + \Gamma_a))^2}\right.$$
$$-\sqrt{(1+n_a)^2(1+2n_s)\Gamma_a + (1+2n_a)(1+n_s)^2\Gamma_s}$$
$$\left.\times\sqrt{(1+2n_s)n_a^2\Gamma_a + (1+2n_a)n_s^2\Gamma_s}\right].$$

Thus concurrence will be given as

$$C(\infty) = \frac{2}{Z_{eq}} \left[|n_s - n_a|(\Gamma_s + \Gamma_a)/2\right.$$
$$-\sqrt{(1+n_a)^2(1+2n_s)\Gamma_a + (1+2n_a)(1+n_s)^2\Gamma_s}$$
$$\left.\times\sqrt{(1+2n_s)n_a^2\Gamma_a + (1+2n_a)n_s^2\Gamma_s}\right]. \tag{3.41}$$

According to Eq. (3.41), significant parameters involved in investigation regarding steady state concurrence are the transition rates (Γ_a and Γ_s) and effective number of photons for super- and sub-radiant states (n_a and n_s) respectively. Simplifying Γ_s, $C(\infty)$ becomes the dimensionless function of Γ_a/Γ_s, n_a and n_s. In order to check the possibility of $C(\infty) > 0$, it is plotted in Fig. 3.3 for different values of n_a and n_s at $\Gamma_a/\Gamma_s \approx 2.8 \times 10^{-4}$.
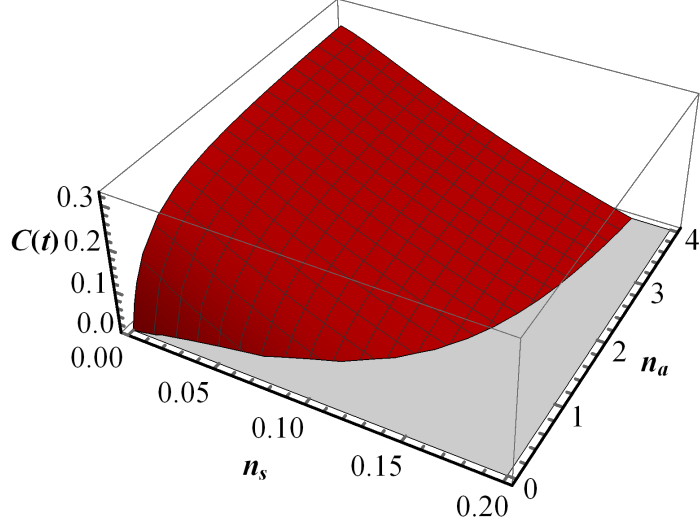
34

Figure 3.3: Steady-state concurrence as a function of n_s and n_a at $\Gamma_a/\Gamma_s \approx 2.8 \times 10^{-4}$.

Fig. 3.3 depicts that $C_{max}(\infty) \approx 0.33$. Another interesting depictions is that at thermal equilibrium ($n_s = n_a$) the concurrence is zero. Thus, entanglement is only possible at out of thermal equilibrium ($n_s \neq n_a$). To further explore the dependence of steady-state concurrence on different parameters, it is plotted (see Fig. 3.4) at $n_s = 10^{-3}$ for different values of Γ_a/Γ_s. It discerns that higher value of concurrence is possible for higher n_a values at smaller Γ_a/Γ_s ratio.
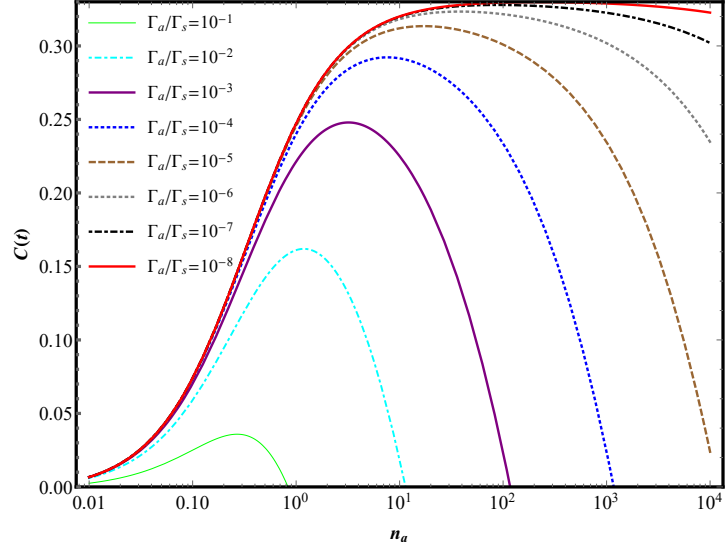
Figure 3.4: Steady-state concurrence as a function of n_a for different values of Γ_a/Γ_s at $n_s = 10^{-3}$.

Chapter 4

Entanglement Dynamics and Superdense Coding Out of Thermal Equilibrium

In this chapter the numerical investigation of entanglement dynamics is done to quantify entanglement for quantum systems out of thermal equilibrium. Because when the density matrix elements out of thermal equilibrium given in Eq. 3.33 are solved at finite time, it give the results that can not be solved analytically. Therefore, we investigate the phenomenon of ESD and SDC, numerically for different initial states. Additionally, the dark period of entanglement and the optimal time for SDC is estimated for each initial state.

In order to examine concurrence at finite time, it can be predicted from Eq. 3.33 that the concurrence is the function of variables such as Γ_a, Γ_s, n_a and n_s. Consequently, for $n_s = 10^{-3}$ the values of n_a and the ratio Γ_a/Γ_s varies from 10^{-1} to 10^4 and 10^{-1} to 10^{-8}, respectively.

4.1 Entangled state

The initially entangled qubits prepared in the state $|\psi\rangle = \sqrt{1-\alpha}\,|G\rangle + \sqrt{\alpha}\,|E\rangle$, where α is the probability amplitude, gives the following initial density matrix

$$\rho(0) = \begin{pmatrix} \alpha & 0 & 0 & \sqrt{\alpha(1-\alpha)} \\ 0 & 0 & 0 & 0 \\ 0 & 0 & 0 & 0 \\ \sqrt{\alpha(1-\alpha)} & 0 & 0 & 1-\alpha \end{pmatrix}. \tag{4.1}$$

37

Using these initial density matrix elements, the time evolution of concurrence ($C(t)$) is plotted in Fig. 4.1 against a probability amplitude ranging from 0 to 1. Two different preferences of $C(t)$ describe the phenomena of ESD ($C_2(t)$) and ESB ($C_1(t)$) after some time. It shows that initially concurrence is not maximum for lower values of α but its dark period is narrow. Lately, concurrence becomes maximum ($\alpha = 0.5$) and then again starts decreasing with increasing α. Also the darker period becomes greater for greater values of α.
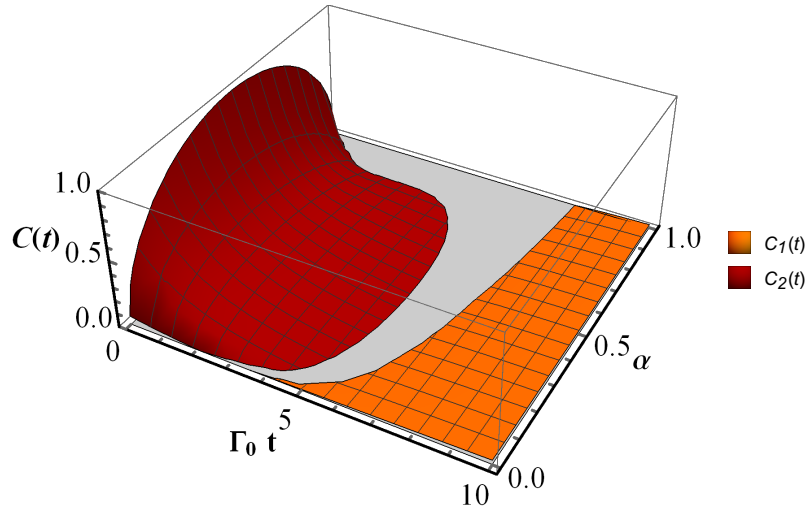
Figure 4.1: (color online) Time variation of concurrence for initially entangled state at $n_a = 10$ and $\Gamma_a/\Gamma_s = 10^{-3}$.

In Fig. 4.2, time evolution of concurrence is plotted for entangled state at $\alpha = 0.5$. We observed that though revival occurs early at higher Γ_a/Γ_s ratio ($\Gamma_a/\Gamma_s = 10^{-1}$) i.e., $t_d = 2.59/\Gamma_0$, but dark period is narrow for lower Γ_a/Γ_s ratio ($\Gamma_a/\Gamma_s = 10^{-3}$) i.e., $t_d = 1.2/\Gamma_0$. Thus, the shorter dark period can be achieved at lower values of Γ_a/Γ_s.
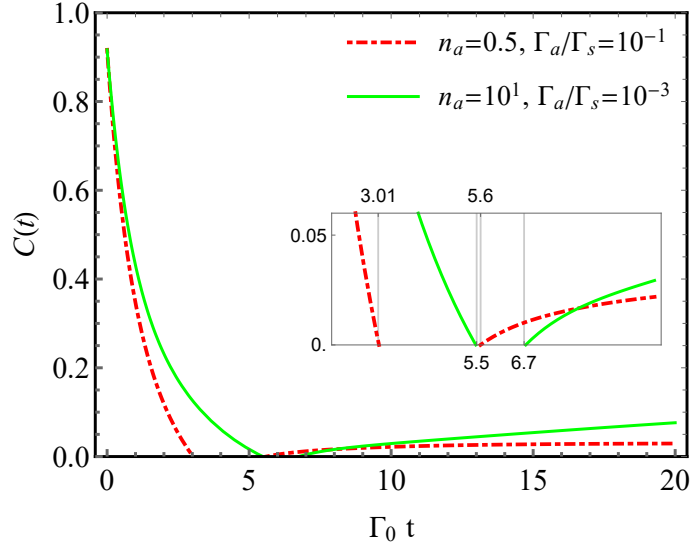
Figure 4.2: (color online) Time variation of concurrence for entangled state at $\alpha = 0.3$.

Furthermore in Fig. 4.3 and Fig. 4.4 time evolution of dense coding capacity is plotted for several value of probability amplitude α and various Γ_a/Γ_s ratios respectively. It is obvious that SDC is not possible for $\alpha = 0$ because it will lead to a pure state. While for $\alpha = 0.5$, state becomes maximally entangled for which dense coding capacity have a maximum possible value $\chi = 2$ (see Fig. 4.3). However, inset of Fig. 4.3 shows that as the degree of entanglement decreases, optimal value of SDC increases making the state more desirable for quantum communication. So, more optimal time is deduced for $\alpha = 0.3$. Thus, in Fig. 4.4 time variation of dense coding capacity for $\alpha = 0.3$ is plotted and evaluated for different values of Γ_a/Γ_s Higher values of super dense capacity are observed with decrease in value of Γ_a/Γ_s. It can be perceived that states with lower transition rate of anti-symmetric than symmetric terms are well considered for optimal superdense coding capacity.
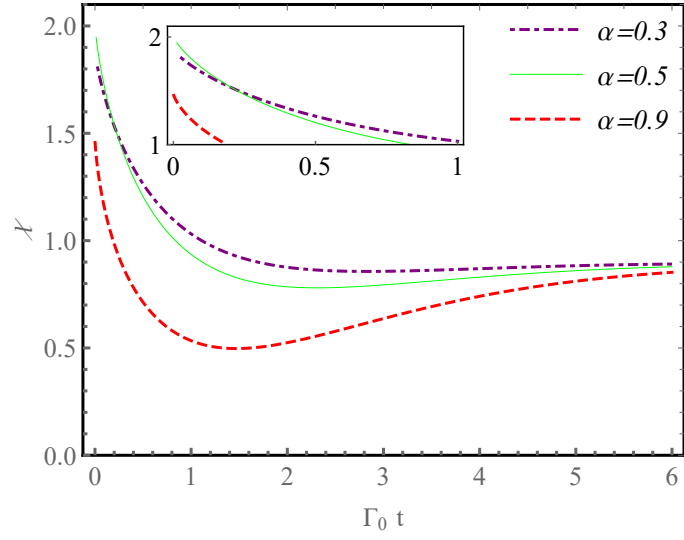
Figure 4.3: Time variation of dense coding capacity χ for entangled state at $n_a = 50$, $\Gamma_a/\Gamma_s = 10^{-4}$, $n_s = 10^{-3}$.
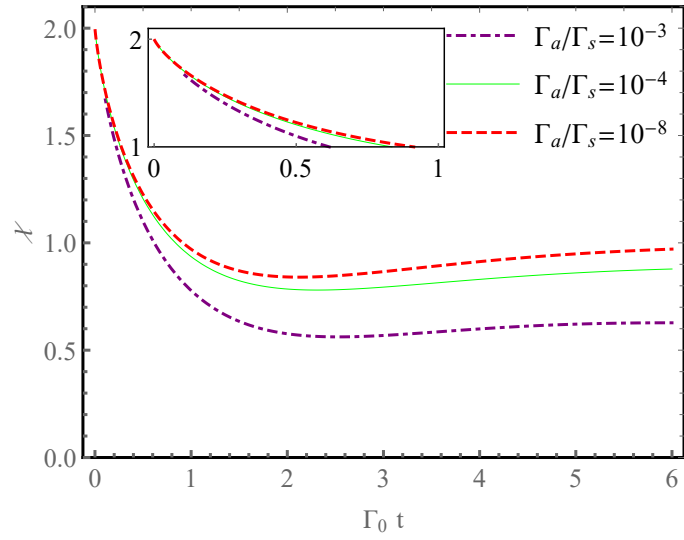

Figure 4.4: Time variation of dense coding capacity χ for entangled state at $n_a = 50$, $\alpha = 0.3$ and $n_s = 10^{-3}$.

4.2 Werner state

Consider the system initially prepared in Werner state $\psi = (1-w)I/4 + w\,|S\rangle\,\langle S|$, where w is the probability amplitude, I is a 4×4 identity matrix and $|S\rangle$ is the symmetric state.

The time variation of concurrence plotted in Fig. 4.5 depicted that the maximum value of concurrence and the shorter dark period is achieved at higher values of probability amplitude w. It also gives the evidence that for the higher value of w first concurrence becomes zero (ESD) and then revives at a later time.

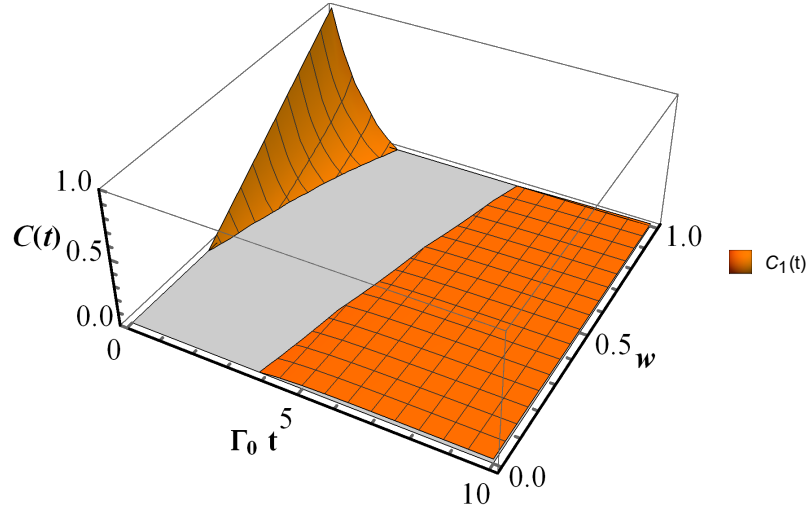

Figure 4.5: (color online) Time variation of concurrence for initially Werner state at $n_a = 0.5$ and $\Gamma_a/\Gamma_s = 10^{-1}$.

Additionally it is obvious from Fig. 4.6 that smaller ratio of Γ_a/Γ_s gives shorter dark period. The inset also shows that the dark period is $t_d \approx 4/\Gamma_0$ for $\Gamma_a/\Gamma_s = 10^{-1}$ and it is $t_d = 3.12/\Gamma_0$ for $\Gamma_a/\Gamma_s = 10^{-4}$.
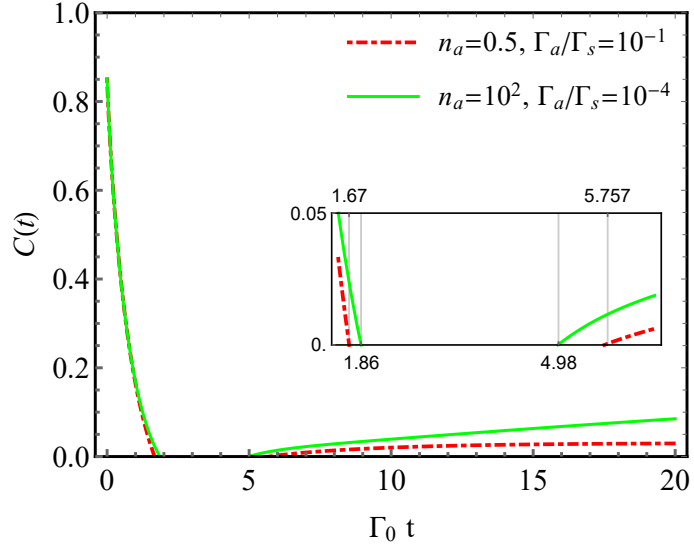
41

Figure 4.6: (color online) Time variation of concurrence for initially Werner state at $w = 0.9$.

Moreover, it is shown that superdense coding is possible for $w > 0.75$ (see Fig. 4.7). It is observed that the optimal time of superdense coding capacity is greater for $w = 0.9$ making the state more feasible for dense coding.
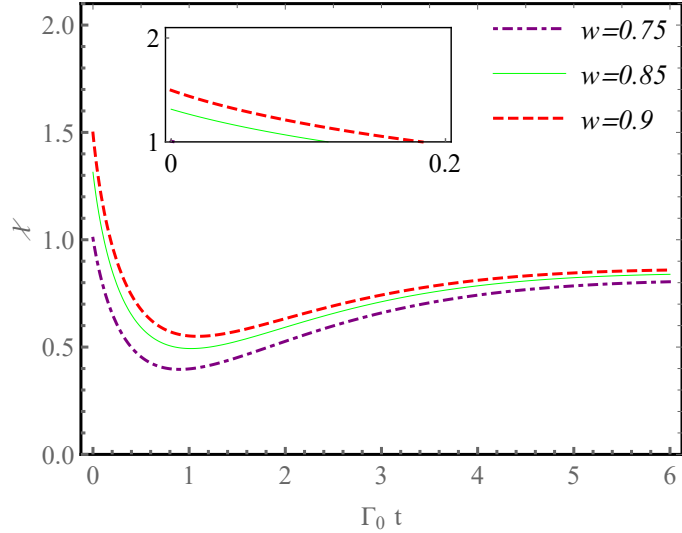

Figure 4.7: Time variation of dense coding capacity χ for Werner state at $\Gamma_a/\Gamma_s = 10^{-4}$, $n_a = 50$ and $n_s = 10^{-3}$.

It is noticed from Fig. 4.8 that the super dense capacity is higher for states that have a higher transition rate of symmetric as compared to antisymmetric state and vice versa.
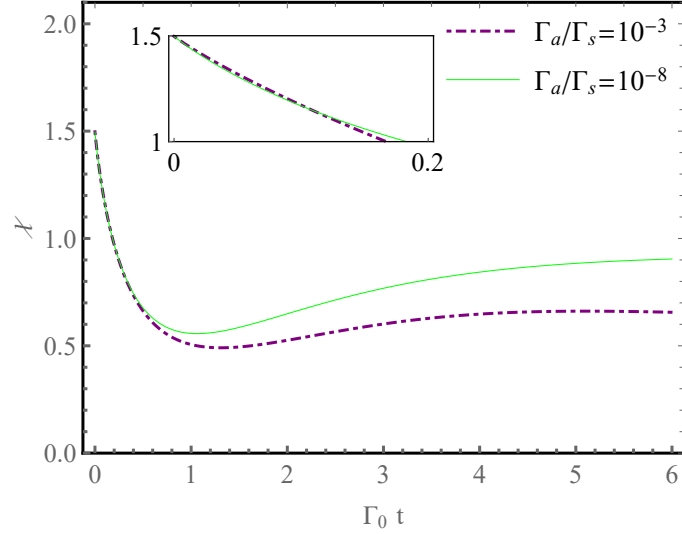

Figure 4.8: Time variation of dense coding capacity χ for Werner state at $w = 0.9$, $n_a = 50$ and $n_s = 10^{-3}$.

4.3   Maximally non-local mixed state (MNMS)

Another important class of X-states is a maximally non-local mixed state (MNMS) which maximally violates CHSH inequalities [56]. Considering the qubits initially prepared as MNMS, the density matrix for this case becomes

$$\rho(0) = \frac{1}{2}\begin{pmatrix} 1 & 0 & 0 & y \\ 0 & 1 & y & 0 \\ 0 & y & 1 & 0 \\ y & 0 & 0 & 1 \end{pmatrix} \tag{4.2}$$

The time evolution of concurrence in Fig. 4.9 predicts the phenomena of ESD $(C_2(t))$ and its rebirth $(C_1(t))$. It also shows that the dark period is shorter for higher probability amplitude y.
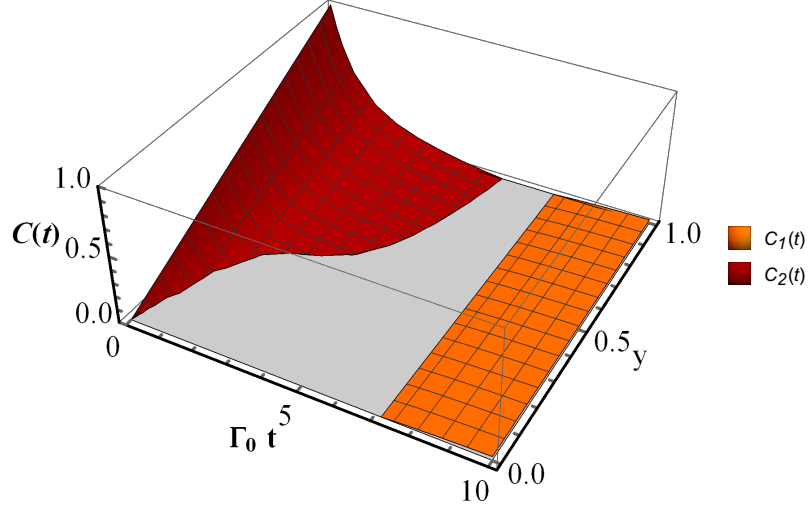
Figure 4.9: (color online) Time variation of concurrence for initially MNMS at $n_a = 10^1$ and $\Gamma_a = 10^{-3}$.

The dependence of concurrence on parameters n_a and Γ_a/Γ_s is depicted in Fig. 4.10. The inset gives the evident that the dark period is broader for a higher Γ_a/Γ_s ratio which is $t_d = 3.25/\Gamma_0$. While for smaller Γ_a/Γ_s ratio the dark period is $t_d = 2.34/\Gamma_0$ which is smaller than prior.
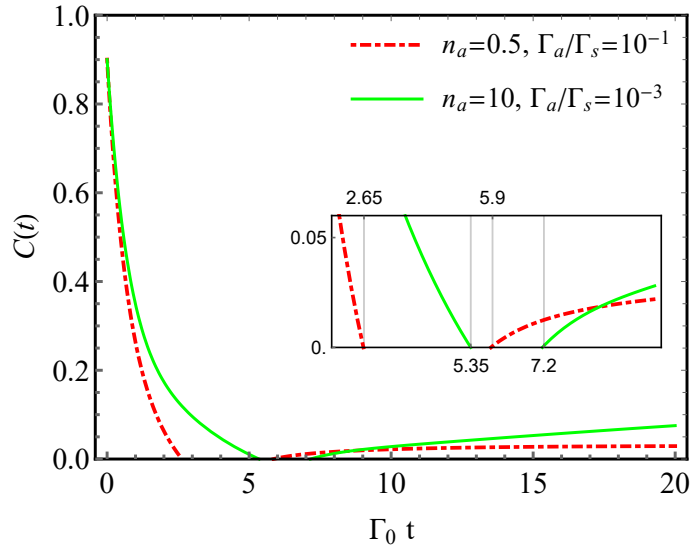

Figure 4.10: (color online) Time variation of concurrence for initially MNMS at $y = 0.9$.

The time evolution of dense coding capacity regarding probability amplitude and Γ_a to Γ_s is plotted in Fig. 4.11 and 4.12, respectively. It can be deduced from results of Fig. 4.11 that dense coding capacity has a greater optimal time for $y = 0.9$. As we move to decrease the probability amplitude, optimal value of SDC decreases making the state less reliable for dense coding as compare to prior one. It is also grasped from Fig. 4.12 that the trend followed in prior states is also valid for MNMS. The smaller the ratio of Γ_a to Γ_s, more significant is the superdense coding capacity.
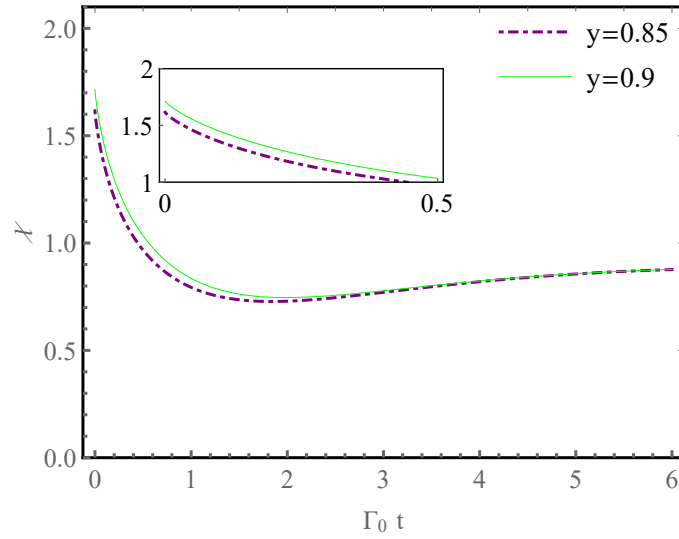

Figure 4.11: Time variation of dense coding capacity χ for MNMS at $\Gamma_a/\Gamma_s = 10^{-4}$, $n_a = 50$ and $n_s = 10^{-3}$.
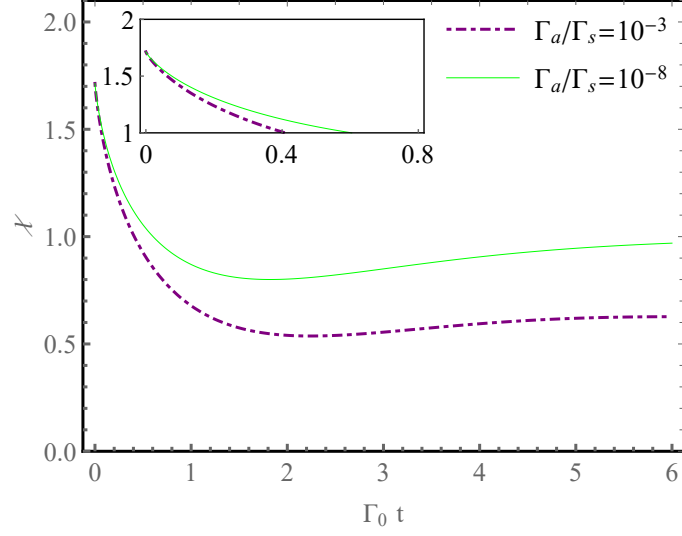
Figure 4.12: Time variation of dense coding capacity χ for MNMS at $y = 0.9$, $n_a = 50$ and $n_s = 10^{-3}$.

4.4 Maximally entangled mixed state (MEMS)

It is a class of X-states that has the maximum degree of entanglement for a given combination of pure states [57]. The density matrix of MEMS for two photon coherence is given as

$$\rho(0) = \begin{pmatrix} x/2 & 0 & 0 & x/2 \\ 0 & 1-x & 0 & 0 \\ 0 & 0 & 0 & 0 \\ x/2 & 0 & 0 & x/2 \end{pmatrix}; 2/3 \leq x \leq 1. \tag{4.3}$$

The time variation of concurrence in Fig. 4.13 predicts ESD because of $C_2(t)$ and its rebirth due to $C_1(t)$. It can be concluded that the entanglement is maximum and the dark period is shorter for greater values of probability amplitude x.

Fig. 4.14 predicts the time evolution of concurrence at different Γ_a/Γ_s values. The inset shows that the dark period for $\Gamma_a/\Gamma_s = 10^{-1}$ is $t_d = 3.2/\Gamma_0$ which is greater than $t_d = 1.75/\Gamma_0$ at $\Gamma_a/\Gamma_s = 10^{-4}$ as predicted.
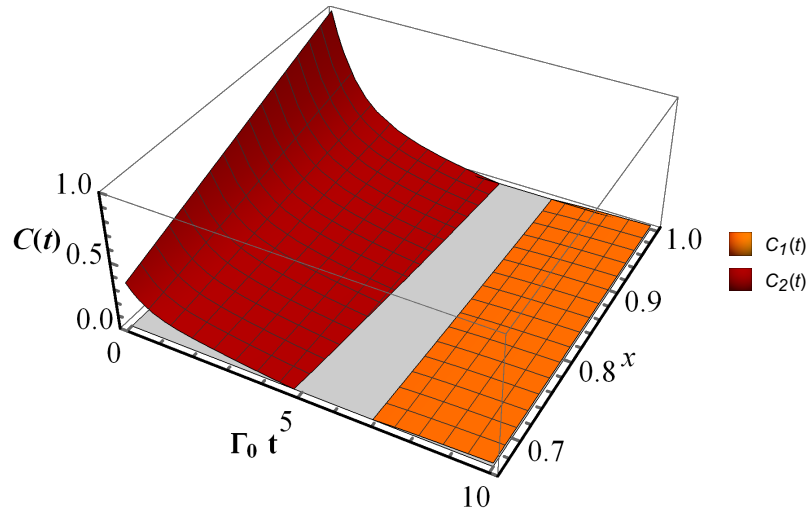
Figure 4.13: (color online) Time variation of concurrence for initially MEMS at $n_a = 10^0$ and $\Gamma_a/\Gamma_s = 10^{-2}$.
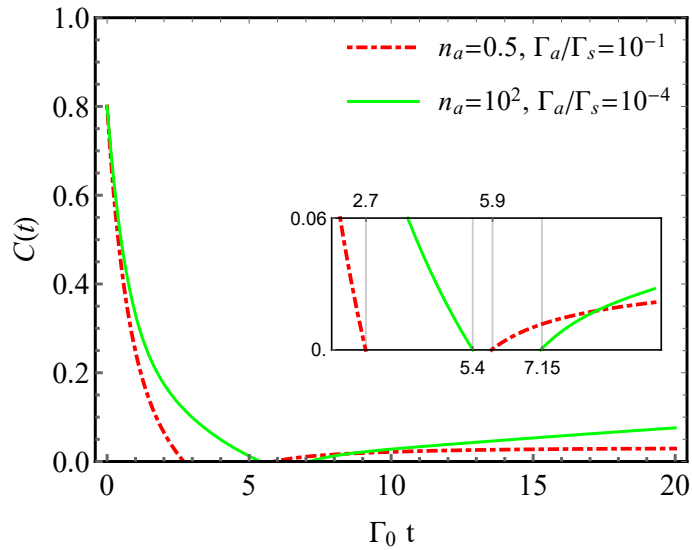
Figure 4.14: (color online) Time variation of concurrence for initially MEMS at $x = 0.9$.

It is evident from Fig. 4.15 that maximum superdense coding is possible for $x = 0.9$ and decreases as we lower the probability amplitude at $\Gamma_0 t = 0$. A state with a higher optimal value and optimal time of SDC is more realistic for quantum communication as compared to others. Inset indicates that the lowest optimal time of SDC is for $x = 0.7$

while the highest is for $x = 0.9$. The time evolution of dense coding capacity plotted in Fig. 4.16 illustrates that optimal value of SDC is greater for lower ratios of Γ_a to Γ_s, supporting the trend of prior states.
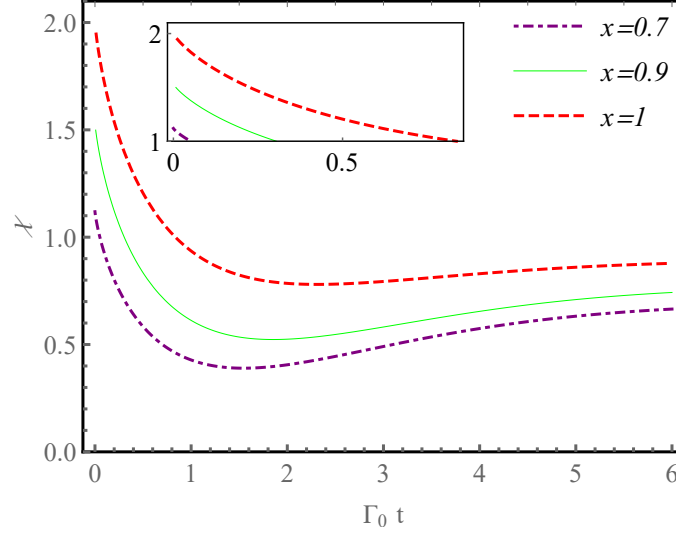

Figure 4.15: Time variation of dense coding capacity χ for MEMS at $\Gamma_a/\Gamma_s = 10^{-4}$, $n_a = 50$ and $n_s = 10^{-3}$.
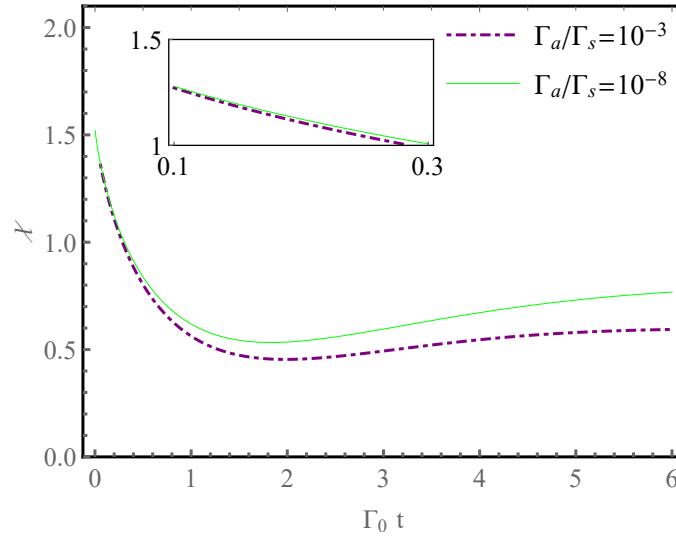

Figure 4.16: Time variation of dense coding capacity χ for MEMS at $x = 0.9$, $n_a = 50$ and $n_s = 10^{-3}$.

Chapter 5

Result and discussion

The objective of this study was the investigation of the phenomena of finite time disentanglement and superdense coding for the quantum system comprised of two quantum emitters placed close to an arbitrary body at a different temperature from its surrounding. To this aim, he Markovian master equation formalism is applied to find rate equations and Wootter's concurrence to interpret the association of transition rates to entanglement sudden death. Then we have simulated the concurrence for different initial X-states. It employs that concurrence varies with the degree of entanglement of the initial state. The presented results also disclosed that dark period becomes narrow for smaller ratio of sub- and super-radiant transition rates implicitly depending on temperature. It also seems that all the states support same trend of results. Further numerical investigation is done to discern the consequence of probability amplitude, super- and sub-radiant transition rates on superdense coding capacity. It is concluded that for lower values of Γ_a/Γ_s superdense coding capacity is greater. This modeled the out-of-thermal equilibrium quantum systems as a good applicant for the early revival of entanglement without any external assistance. Furthermore, our findings make these quantum systems an attractive candidate for quantum information technologies.

Bibliography

[1] J. R. Taylor and J. R. Taylor, *Classical mechanics*, vol. 1. Springer, 2005.

[2] T. Bécherrawy, *Electromagnetism: Maxwell equations, wave propagation and emission*. John Wiley & Sons, 2013.

[3] G. N. Lewis and M. Randall, *Thermodynamics*. No. 44, Krishna Prakashan Media, 1963.

[4] F. K. Richtmyer, E. H. Kennard, and J. N. Cooper, *Introduction to modern physics*, vol. 747. McGraw-Hill New York, 1955.

[5] A. I. Miller, *Albert Einstein's Special Theory of Relativity: emergence (1905) and early interpretation (1905-1911)*. Springer, 1981.

[6] R. A. Serway and J. W. Jewett, *Physics for scientists and engineers*. Cengage learning, 2018.

[7] R. Loudon, *The quantum theory of light*. OUP Oxford, 2000.

[8] H. Kragh, *Niels Bohr and the quantum atom: The Bohr model of atomic structure 1913-1925*. OUP Oxford, 2012.

[9] G. N. Lewis, "The conservation of photons," *Nature*, vol. 118, no. 2981, pp. 874–875, 1926.

[10] D. H. Menzel, *Fundamental formulas of physics*, vol. 1. Courier Corporation, 1960.

[11] H. S. Green and M. Born, "Matrix mechanics," *(No Title)*, 1965.

[12] D. J. Griffiths and D. F. Schroeter, *Introduction to quantum mechanics*. Cambridge university press, 2018.

[13] S. WIGGINS, "Elementary quantum mechanics," 2020.

[14] C. Itzykson and J.-B. Zuber, *Quantum field theory*. Courier Corporation, 2012.

[15] A. Einstein, B. Podolsky, and N. Rosen, "Can quantum-mechanical description of physical reality be considered complete?," *Physical review*, vol. 47, no. 10, p. 777, 1935.

[16] C. Gerry and P. L. Knight, *Introductory quantum optics*. Cambridge university press, 2005.

[17] J. R. Klauder and B.-S. Skagerstam, *Coherent states: applications in physics and mathematical physics*. World scientific, 1985.

[18] P. G. Kryukov, "Ultrashort-pulse lasers," *Quantum electronics*, vol. 31, no. 2, p. 95, 2001.

[19] H. A. Haus, "Mode-locking of lasers," *IEEE Journal of Selected Topics in Quantum Electronics*, vol. 6, no. 6, pp. 1173–1185, 2000.

[20] J. J. Degnan, "Theory of the optimally coupled q-switched laser," *IEEE Journal of Quantum Electronics*, vol. 25, no. 2, pp. 214–220, 1989.

[21] R. Horodecki, P. Horodecki, M. Horodecki, and K. Horodecki, "Quantum entanglement," *Reviews of modern physics*, vol. 81, no. 2, p. 865, 2009.

[22] J. G. Brookshear, *Computer science: An overview*. Benjamin-Cummings Publishing Co., Inc., 1991.

[23] E. Turban, R. K. Rainer, R. E. Potter, *et al.*, *Introduction to information technology*. John Wiley & Sons New York, NY, 2001.

[24] M. A. Nielsen and I. L. Chuang, *Quantum information and quantum computation*. Cambridge university press Cambridge, 2000.

[25] A. K. Ekert, "Quantum cryptography based on bell's theorem," *Physical review letters*, vol. 67, no. 6, p. 661, 1991.

[26] C. E. Shannon, "Communication theory of secrecy systems," *The Bell system technical journal*, vol. 28, no. 4, pp. 656–715, 1949.

[27] C. H. Bennett, G. Brassard, C. Crépeau, R. Jozsa, A. Peres, and W. K. Wootters, "Teleporting an unknown quantum state via dual classical and einstein-podolsky-rosen channels," *Physical review letters*, vol. 70, no. 13, p. 1895, 1993.

[28] J.-W. Pan, D. Bouwmeester, H. Weinfurter, and A. Zeilinger, "Experimental entanglement swapping: entangling photons that never interacted," *Physical review letters*, vol. 80, no. 18, p. 3891, 1998.

[29] C. H. Bennett and S. J. Wiesner, "Communication via one-and two-particle operators on einstein-podolsky-rosen states," *Physical review letters*, vol. 69, no. 20, p. 2881, 1992.

[30] T. Yu and J. Eberly, "Finite-time disentanglement via spontaneous emission," *Physical Review Letters*, vol. 93, no. 14, p. 140404, 2004.

[31] T. Yu and J. Eberly, "Sudden death of entanglement," *Science*, vol. 323, no. 5914, pp. 598–601, 2009.

[32] F. Wang, P.-Y. Hou, Y.-Y. Huang, W.-G. Zhang, X.-L. Ouyang, X. Wang, X.-Z. Huang, H.-L. Zhang, L. He, X.-Y. Chang, *et al.*, "Observation of entanglement sudden death and rebirth by controlling a solid-state spin bath," *Physical Review B*, vol. 98, no. 6, p. 064306, 2018.

[33] Z. Ficek and R. Tanaś, "Dark periods and revivals of entanglement in a two-qubit system," *Physical Review A*, vol. 74, no. 2, p. 024304, 2006.

[34] C.-J. Yang, J.-H. An, W. Yang, and Y. Li, "Generation of stable entanglement between two cavity mirrors by squeezed-reservoir engineering," *Physical Review A*, vol. 92, no. 6, p. 062311, 2015.

[35] A. Pedram and Ö. E. Müstecaplıoğlu, "An overview: Steady-state quantum entanglement via reservoir engineering," *arXiv preprint arXiv:2303.00490*, 2023.

[36] P. G. Kwiat, S. Barraza-Lopez, A. Stefanov, and N. Gisin, "Experimental entanglement distillation and 'hidden'non-locality," *Nature*, vol. 409, no. 6823, pp. 1014–1017, 2001.

[37] S. Maniscalco, F. Francica, R. L. Zaffino, N. L. Gullo, and F. Plastina, "Protecting entanglement via the quantum zeno effect," *Physical review letters*, vol. 100, no. 9, p. 090503, 2008.

[38] G. S. Agarwal, "Quantum statistical theories of spontaneous emission and their relation to other approaches," *Quantum Optics*, pp. 1–128, 2006.

[39] Z. Ficek and S. Swain, *Quantum interference and coherence: theory and experiments*, vol. 100. Springer Science & Business Media, 2005.

[40] K. Almutairi, R. Tanaś, and Z. Ficek, "Generating two-photon entangled states in a driven two-atom system," *Physical Review A*, vol. 84, no. 1, p. 013831, 2011.

[41] D. Sych and G. Leuchs, "A complete basis of generalized bell states," *New Journal of Physics*, vol. 11, no. 1, p. 013006, 2009.

[42] M. Koashi and M. Ueda, "Reversing measurement and probabilistic quantum error correction," *Physical review letters*, vol. 82, no. 12, p. 2598, 1999.

[43] A. Carvalho, A. Reid, and J. Hope, "Controlling entanglement by direct quantum feedback," *Physical Review A*, vol. 78, no. 1, p. 012334, 2008.

[44] J.-C. Lee, H.-T. Lim, K.-H. Hong, Y.-C. Jeong, M. Kim, and Y.-H. Kim, "Experimental demonstration of delayed-choice decoherence suppression," *Nature Communications*, vol. 5, no. 1, p. 4522, 2014.

[45] L. Viola, E. Knill, and S. Lloyd, "Dynamical decoupling of open quantum systems," *Physical Review Letters*, vol. 82, no. 12, p. 2417, 1999.

[46] D. A. Lidar, I. L. Chuang, and K. B. Whaley, "Decoherence-free subspaces for quantum computation," *Physical Review Letters*, vol. 81, no. 12, p. 2594, 1998.

[47] Z. Ficek and R. Tanaś, "Delayed sudden birth of entanglement," *Physical Review A*, vol. 77, no. 5, p. 054301, 2008.

[48] C. H. Bennett, H. J. Bernstein, S. Popescu, and B. Schumacher, "Concentrating partial entanglement by local operations," *Physical Review A*, vol. 53, no. 4, p. 2046, 1996.

[49] S. Hill, "Phys. rev. lett., 78(1997) 5022; wootters w. k.," *Phys. Rev. Lett.*, vol. 80, p. 2245, 1998.

[50] W. An-Min, "A simplified and obvious expression of concurrence in wootters' measure of entanglement of a pair of qubits," *Chinese physics letters*, vol. 20, no. 11, p. 1907, 2003.

[51] B. Bellomo, R. Lo Franco, and G. Compagno, "Long-time preservation of nonlocal entanglement," *Advanced Science Letters*, vol. 2, no. 4, pp. 459–462, 2009.

[52] T. Yu and J. Eberly, "Quantum inf. comput. 7 (2007) 459; q. chen, c. zhang, s. yu, xx yi, ch oh," *Phys. Rev. A*, vol. 84, p. 042313, 2011.

[53] B. Bellomo and M. Antezza, "Creation and protection of entanglement in systems out of thermal equilibrium," *New Journal of Physics*, vol. 15, no. 11, p. 113052, 2013.

[54] B. Bellomo and M. Antezza, "Steady entanglement out of thermal equilibrium," *Europhysics Letters*, vol. 104, no. 1, p. 10006, 2013.

[55] R. H. Dicke, "Coherence in spontaneous radiation processes," *Physical review*, vol. 93, no. 1, p. 99, 1954.

[56] J. F. Clauser, M. A. Horne, A. Shimony, and R. A. Holt, "Proposed experiment to test local hidden-variable theories," *Physical review letters*, vol. 23, no. 15, p. 880, 1969.

[57] S. Ishizaka and T. Hiroshima, "Maximally entangled mixed states under nonlocal unitary operations in two qubits," *Physical Review A*, vol. 62, no. 2, p. 022310, 2000.